ADVANCED ENERGY MATERIALS
www.advenergymat.de

Ethylene Electrosynthesis via Selective CO_2 Reduction: Fundamental Considerations, Strategies, and Challenges

Thomas O' Carroll, Xiaoxuan Yang, Kenneth J. Gordon, Ling Fei, and Gang Wu**

The electrochemical carbon dioxide reduction reaction (CO_2RR) is a promising approach for reducing atmospheric carbon dioxide (CO_2) emissions, allowing harmful CO_2 to be converted into more valuable carbon-based products. On one hand, single carbon (C_1) products have been obtained with high efficiency and show great promise for industrial CO_2 capture. However, multi-carbon (C_{2+}) products possess high market value and have demonstrated significant promise as potential products for CO_2RR. Due to CO_2RR's multiple pathways with similar equilibrium potentials, the extended reaction mechanisms necessary to form C_{2+} products continue to reduce the overall selectivity of CO_2-to-C_{2+} electroconversion. Meanwhile, CO_2RR as a whole faces many challenges relating to system optimization, owing to an intolerance for low surface pH, systemic stability and utilization issues, and a competing side reaction in the form of the H_2 evolution reaction (HER). Ethylene (C_2H_4) remains incredibly valuable within the chemical industry; however, the current established method for producing ethylene (steam cracking) contributes to the emission of CO_2 into the atmosphere. Thus, strategies to significantly increase the efficiency of this technology are essential. This review will discuss the vital factors influencing CO_2RR in forming C_2H_4 products and summarize the recent advancements in ethylene electrosynthesis.

1. Introduction

The effect of widespread carbon dioxide (CO_2) emissions has been extensively studied by researchers worldwide, who have nearly all agreed that the excessive use of fossil fuels has had a direct impact on the environment and climate.[1,2] While significant progress has been made, there is still a daunting amount of research, work, and adaptation to be done if this crisis is to be contained. Naturally, much of this responsibility falls to scientists and engineers to develop novel strategies that preserve modern conveniences and provide an optimistic future for the world. In terms of the carbon dioxide reduction reaction (CO_2RR), reducing the CO_2 in the environment is crucial in and of itself, but it is also critical that products of high value are generated to entice industry members to use this technology.[3,4] To this end, the production of multi-carbon (C_{2+}) products via CO_2RR has become a promising approach to meet the challenges presented by climate change.[5–7] C_{2+} products like ethylene (C_2H_4) and ethanol (C_2H_5OH) boast numerous well-established applications and a high energy density, which drives up their market value in comparison to single carbon (C_1) products like carbon monoxide (CO) and formic acid (HCOOH).[3,8] Currently, many high-performance catalysts are effective for producing C_1 products;[9–11] if C_{2+}-selective catalysts could achieve similarly high benchmarks, then CO_2RR-to-C_{2+} would undoubtedly be more desirable due to the quality of the products.[12,13]

This review will focus primarily on ethylene as a target product for a variety of reasons. Among C_{2+} products, ethylene (i) possesses a more established use for industrial applications,[14] (ii) is the C_{2+} product formed in the highest quantity on most copper (Cu) catalysts,[15,16] and (iii) benefits from less costly and higher efficiency downstream separation processes compared other C_{2+} products like ethanol, n-propanol, and acetate.[17,18] These aspects currently distinguish ethylene-selective electrocatalysts as an appropriate option for future industrial application of CO_2RR toward forming C_{2+} products. Despite Cu being the only effective element for reliably producing high quantities of C_{2+} products, a staggering amount of novel strategies and catalyst designs have been created for realizing high-efficiency ethylene production.[19,20] Throughout the rest of this report, we will review proposed industrial requirements for electrochemical CO_2RR toward ethylene and discuss how the performance of state-of-the-art electrocatalysts compares to these requirements. Subsequently, the fundamental considerations critical to understanding CO_2RR, specifically ethylene selective CO_2RR, will be covered. Additionally, the equipment used for conducting CO_2RR will be reviewed, and the efficacy of the reactors, protocols,

T. O' Carroll, X. Yang, G. Wu
Department of Chemical and Biological Engineering
University at Buffalo
The State University of New York
Buffalo, NY 14260, USA
E-mail: gangwu@buffalo.edu
K. J. Gordon, L. Fei
Department of Chemical Engineering
Institute for Materials Research and Innovations
University of Louisiana at Lafayette
Lafayette, LA 70504, USA
E-mail: ling.fei@louisiana.edu

The ORCID identification number(s) for the author(s) of this article can be found under https://doi.org/10.1002/aenm.202401558

DOI: 10.1002/aenm.202401558

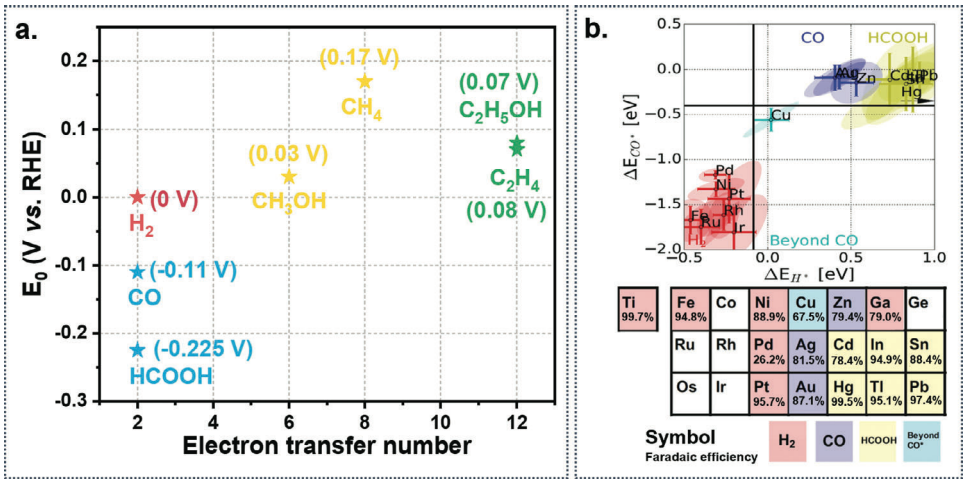

Figure 1. a) Graphical depiction of the theoretical equilibrium potentials for processes relevant to CO_2RR. b) Top: adsorption energy comparison between *CO and *H across metals used for CO_2RR. Bottom: reformatted periodic table highlighting metals used for CO_2RR, coloring each based on their dominant product. Reproduced with permission.[50] Copyright 2017, Wiley.

membranes, electrolytes, and diffusion layers will be evaluated. Following this discussion, we will analyze the logistical importance of ethylene within a global economy and compare its financial incentives with other CO_2RR products before identifying area where CO_2-to-C_2H_4 catalysts need to improve for industrial viability. Finally, promising strategies related to catalyst and reactor design developed by researchers will be summarized before discussing CO_2RR's grand challenges. The aim of this review is to provide readers with an up-to-date, holistic understanding of ethylene electrosynthesis via CO_2RR by discussing each factor within the process, ranging from the minutia of catalyst design to industrial implementation. A comprehensive literature review has been conducted on each of these factors, which have been dissected and assessed accordingly. Particularly, we wish to illustrate how the catalyst perspective and system perspective interact with each other to realize high-efficiency ethylene synthesis.

2. Fundamental Considerations for CO_2RR: A Catalyst Perspective

The primary concerns for reaction are the mass transfer behavior of the reacting species to and from the active sites, and the kinetic and thermodynamic energy barriers. CO_2RR is a multipathway reaction with many different steps and intermediates, drastically complicating the steering of the reaction toward more desired products (**Figure 1a**).[14,21–25] Tuning the selectivity is the primary challenge for CO_2RR from a reaction engineering perspective; the sheer volume of pathways that share a very narrow potential window causes serious issues that are not as pronounced in many other catalytic systems.[26] The key issue that makes CO_2RR-to-C_{2+} so much more complicated than CO_2RR-to-C_1 is that the catalyst must satisfy the need to form both C_1 intermediates and combine them in the C-C coupling step. The precise mechanism of how this combination occurs is not easily determined, as it varies significantly from catalyst to catalyst, especially concerning which C_1 intermediates are combined in the most thermodynamically favorable way.[15,27,28] Fundamentally, however, CO_2-to-C_2H_4 conversion should be understood in this context, which is to say that CO_2 is adsorbed, reduced, coupled, and desorbed as a C_{2+} product. Naturally, complications arise when considering how the adsorption and the surface/reactant interactions affect the intermediates formed and, ultimately, the products obtained.[29] A fundamental challenge with reactions similar to CO_2RR lies in breaking the so-called linear-scaling relationship, which describes how catalysts bind intermediates of different adsorption energies.[30,31] In principle, the binding energy of the surface affects all intermediates within the reaction, which is incredibly challenging for CO_2RR due to the multitude of species on the surface.[32,33] The underlying mechanism taking place that causes this behavior is related to the similarity between the intermediates. In principle, each of the intermediates within the CO_2-to-C_2H_4 reaction pathway are chemically similar, since each contains the same subset of atoms. The material in the catalyst has an affinity for each of these atoms, and while the strength may vary slightly depending on the specific intermediate, overall this variation has little impact on the behavior.[30] In fact, this phenomenon can be extended to atoms of different types, since the characteristics of a material that cause high adsorption strength for C in *CO are the same characteristics that cause high adsorption of undesirable species like *H.[32,34] For example, for particularly strongly adsorbing transition metals like Fe, CO_2RR is highly inefficient due to the adsorption of both carbonaceous intermediates and protons.[33] On the other hand, Ni functions very well as a catalyst for producing CO due to its weak adsorption for all *C_1 species and protons, allowing the reactant to easily desorb before it is excessively reduced to methanol or methane.[32] Driving high selectivity for certain products can be incredibly challenging since adsorption strength plays a crucial role in the selectivity of the process for each step. Significant effort has been devoted to breaking the linear scaling relationship for many electrochemical reactions, like the oxygen evolution reaction (OER),[35,36] oxygen reduction reaction (ORR),[37] or electrochemical NH_3 synthesis, producing promising results.[34,38,39] The next generation of high-performance CO_2RR catalysts must find new ways to alter the adsorption characteristics of the catalyst to control the selectivity as much as possible. Currently,

techno-economic analyses (TEAs) suggest an industrial goal for ethylene selectivity of ≈90% Faradaic efficiency (FE), which has yet to be achieved.[8,14,40] Top-performing catalysts have shown ethylene FEs within ≈5% of this goal.[41,42]

The first impediment a CO_2RR catalyst faces is the activation of $*CO_2$, which is a stable molecule owing to its lack of an obvious axis for reaction yet does not limit the formation of C_2 products despite requiring significant overpotential.[22,43] Following the protonation and reduction of $*CO_2$, *CO is formed in a rather direct, relatively easily controlled process. This behavior depends on the configuration of the $*CO_2^-$, since it can either be adsorbed by the C or the O atoms, with the former leading to *CO and the latter leading to HCOOH.[44,45] Therefore, products like CO and HCOOH can be obtained with very high FEs, requiring a 2-electron transfer reaction pathway and lower energy requirement. Thus, catalysts with relatively low adsorption strength for $*C_1$ intermediates can be used to their fullest potential at low voltage.[46] In this way, products quickly desorb from the catalyst's surface, hydrogen evolution reaction (HER) side reaction can be inhibited effectively by maintaining low overpotential, and intermediate interactions are very limited, preventing C_{2+} formation. These conditions can lead to high FEs of >95% for lightly reduced C_1 products, making them the most appropriate catalysts for CO_2 electroconversion.[47,48] In essence, CO-selective catalyst design benefits from a low concern for selectivity, aside from preventing the formation of H_2 via HER.[12,49]

On the other hand, if these 2-electron products are still adsorbed to the surface, additional reactions that lead to highly reduced C_1 and C_{2+} products may occur. When examining the formation of C_{2+} pathways, the reaction mechanisms may diverge significantly at this point because some catalysts may preferentially form further reduced $*C_1$ intermediates before the C-C coupling step, such as *CHO, *COH, or $*CH_2$.[22,51] Meanwhile, other catalysts may quickly combine *CO to form *OCCO. It has been suggested that the initial $*C_2$ intermediate may impact the overall reaction pathway when forming C_{2+} products.[21,52] Controlling the precise $*C_1$ intermediates formed is difficult and only observable experimentally through advanced in situ characterization techniques. For this reason, most catalysts will produce multiple types of $*C_1$ intermediates at a time since there usually is not a favorable pathway.[5] However, *CO is nearly always considered the dominant $*C_1$ intermediate due to thermodynamic barriers toward forming *CHO or *COH.[22] In some instances, it has been found that the formation of hydrogenated $*C_1$ intermediates can limit the reaction, particularly when comparing the formation of *CHO versus *COH.[53,54] Even still, the formation of more heavily reduced $*C_1$ intermediates like $*CH_2$ is exceedingly rare on C_{2+} selective catalysts, since this behavior implies that the catalyst may not have sufficient intermediate mobility or $*C_1$ concentration, thereby hampering the C-C coupling rate.

Once these slightly reduced $*C_1$ intermediates begin to form, the selectivity of the catalyst becomes much more difficult to control for many reasons. These intermediates will lead to either heavily reduced $*C_1$ products like methane or methanol or combine to form C_{2+} products, mainly depending on the intermediate coverage, mobility, and overpotential.[22,55–57] Nearly all products that require repeated reduction steps struggle with substantial selectivity problems. To illustrate this phenomenon, CO_2RR to CH_4 is an 8-electron transfer reaction pathway, which requires a high concentration of protons at the catalyst/electrolyte interface, higher overpotentials, and stronger adsorption strength.[58–61] This is necessary for all highly reduced products, including every C_{2+}, which is the root cause of the selectivity problem for CO_2RR.[53] These conditions reduce the selectivity for specific CO_2RR products by (i) decreasing the amount of thermodynamically prohibitive pathways, (ii) reducing the selectivity of CO_2RR itself in favor of HER, and (iii) placing higher stress on the catalyst's (and the system components') durability.

The second concern after the initial adsorption and activation of CO_2 molecules is the C-C coupling step, which involves the interaction of two $*C_1$ intermediates to form a $*C_2$ intermediate. This step is nearly always the limiting step for the CO_2RR process due to a high energy barrier for the reaction itself and the need for sufficient surface CO_2 concentration and $*C_1$ coverage,[24,62] not to mention guiding the process toward a specific C_{2+} product.[22] An increased surface concentration of $*C_1$ intermediates increases the chances of interaction between them,[55] which suggests that a low desorption rate of these C_1 intermediates is desirable. There are multiple methods for increasing the surface concentration of $*C_1$ intermediates like *CO, such as the inclusion of ligands, polymers, and other species to help entrap the *CO.[16,63–66] On top of that, low $*C_1$ concentration at the surface can promote HER side reaction, reducing the overall selectivity of the catalyst for CO_2RR in general.[21,67,68] Regrettably, the matter is not simply solved by using a catalyst with very high adsorption for $*C_1$ intermediates due to the need for these intermediates to be able to freely move around the surface of the catalyst. Thus, high adsorption strength will ultimately result in reduced C-C coupling rate due to infrequent $*C_1$ interaction, thereby promoting the formation of highly reduced C_1 products. It has been suggested that one of the best ways for C-C coupling to be encouraged is by incorporating adsorption strength gradients on the surface of the catalyst, further emphasizing the importance of a well-controlled reaction interface. These adsorption strength gradients can be present due to the formation of different surface morphologies, such as roughness,[69,70] defects and vacancies,[42] differing crystallographic domains,[27,71] nanostructuring,[72–75] or surface modifications through the usage of dopants.[15,41,54,76] The underlying principle behind this phenomena lies in the formation of an axis that encourages the movement and interaction of $*C_1$ species at the surface, thus enhancing the rate of $*C_2$ formation.[27,42]

In all, the adsorption properties of the catalyst surface needs to be neither too strong nor too weak to best encourage the formation of C_{2+}; copper (Cu) happens to possess an adsorption strength for these intermediates that is appropriate for this application, which is why it is by far the most effective active material for CO_2RR toward C_{2+} (Figure 1b).[5,50,77] In this way, a diverse set of possible adsorbed intermediate configurations can be present on the surface of Cu, which directly impacts the selectivity of the overall reaction. Based on *operando* Raman spectroscopy information obtained on Cu (100), it has been observed that the ratio of two *CO-related peaks can describe the amount and quality of adsorbed CO species on the surface of the catalyst (**Figure 2a**).[55] When the ratio between the peak intensity of the CO rotation band and the Cu-CO stretching band was maximized, ethylene formation was increased. According to accompanying density-functional theory (DFT) calculations, the

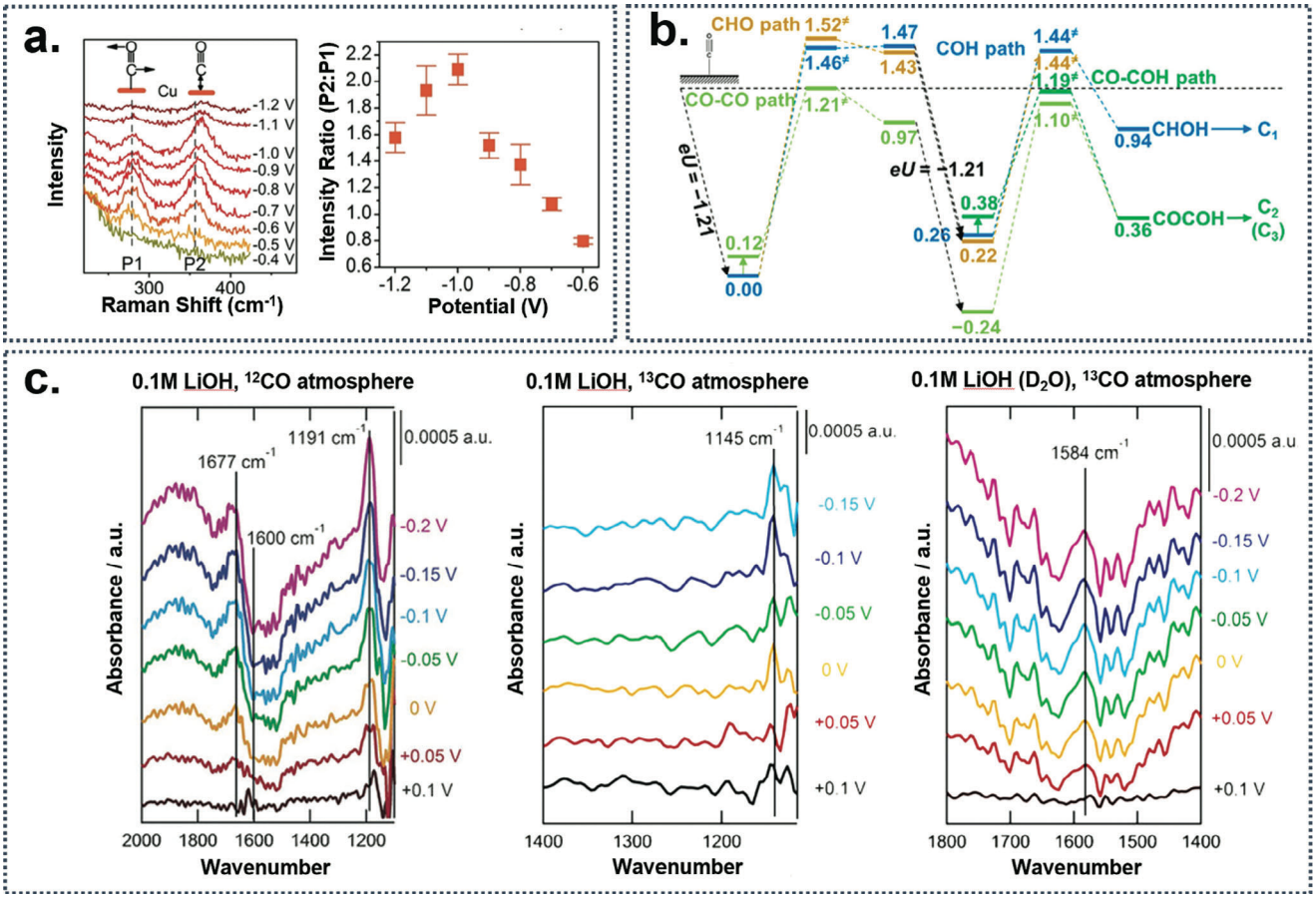

Figure 2. a) Left: presentation of the Raman spectroscopy peaks associated with *CO (P1 and P2) observed in an in situ Raman spectroscopy experiment on a Cu-based catalyst. Right: intensity ratio of P2:P1 for the Cu-based catalyst at different potentials. Reproduced with permission.[55] Copyright 2021, American Chemical Society. b) Free-energy diagram for the progression of CORR at pH = 12, with the CO-CO pathway being dominant. Reproduced with permission.[78] Copyright 2016, American Chemical Society. c) In situ Raman spectroscopy data elucidating the intermediates formed during CORR at different potentials. Left: peaks associated with CO stretching (1677 cm^{-1}), OH bending (1600 cm^{-1}), and C-OH stretching (1191 cm^{-1}). Middle: evaluation under ^{13}CO atmosphere, showing a C-OH stretching band at 1145 cm^{-1}. Right: formation of an unknown peak at 1584 cm^{-1}, which was assigned to OCCOH stretching. Reproduced with permission.[79] Copyright 2017, Wiley.

underlying cause of this behavior is an increase in the quantity of $*CO^{atop}$ compared to $*CO^{bridge}$, resulting in more easily coupled $*C_1$ intermediate species. Such behavior is only possible under optimal adsorption conditions, promoting the usage of Cu over other materials for C_{2+} formation.

Researchers conducting DFT studies and in situ observational techniques have proposed numerous reaction pathways. As an example, *CHO may often form the *CHOH intermediate, which prefers to form heavily reduced C_1 products rather than C_{2+} (Figure 2b).[78] However, most researchers agree that the reaction pathway toward ethylene on a generic Cu (100) surface proceeds via the formation *OCCOH, whether it originates from the dimerization of *CO or the combination of *CO and *COH. Experimentally, in situ Raman spectroscopy data was obtained for the carbon monoxide reduction reaction (CORR) over Cu (100), which showed stretching bands associated with *COH and *OCCOH at very low overpotentials (Figure 2c).[79] In agreement with many computational models developed for CO_2RR and CORR, *CHO was not observed within this experiment, as *CHO is generally considered to have a higher thermodynamic energy requirement when compared to the formation of *COH. In contrast, a recent study by Li et al. demonstrates a method for enabling customizable C_{2+} selectivity based on the *O interaction strength at the surface of the catalyst.[80] The researchers posit that the late-stage 11-electron-transferred C_{2+} intermediate $*CH_2CHO$ shows control over the ratio of ethylene to ethanol if the O atom can be anchored or repelled from the surface. By doping a Cu-based catalyst with different species, they uncovered a volcano-plot distribution when comparing the ethylene to ethanol ratio with the *O adsorption strength of the doping species.[80] While the formation of a CHO structure (whether in the form of *CHO or $*CH_2CHO$) is not typically considered to be thermodynamically favorable, it could be that atoms with high O affinity anchor the O atom in *CO at the surface.[81] Conventionally, *CO is thought to interact with the surface only by the C atom, but if instead the *CO is adsorbed flat on the surface, perhaps this alternate mechanism is promoted.[80] Other research has echoed this sentiment, suggesting that depending on the catalyst, the formation of *CHO is not as unfavorable as many believe.[81–84]

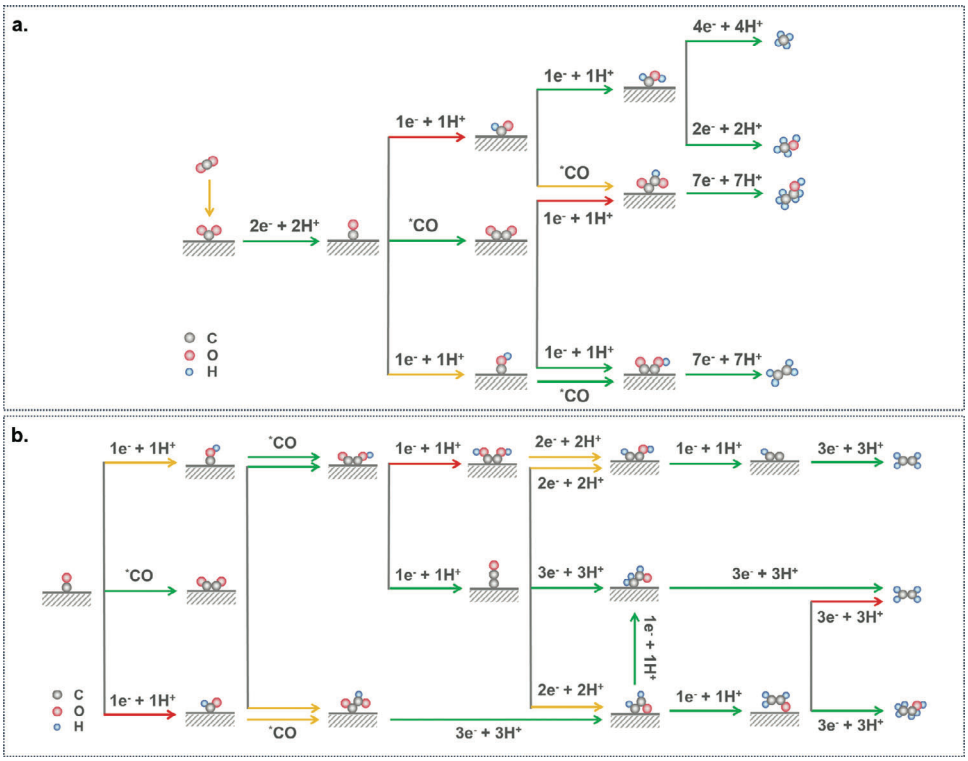

Figure 3. a) Possible CO_2RR mechanism relying on early pathway bifurcation between ethylene and ethanol. b) Possible CORR mechanism relying on later-stage bifurcation routes between ethylene and ethanol. Green, Yellow, and Red arrows indicate the plausibility of the particular reaction pathway.

Still, under high pH and middling potential application, *CO dimerization remains the most commonly accepted coupling mechanism before further protonation to *OCCOH. In either case, it's typically thought that *CCO or *HOCCOH is formed following *OCCOH,[79,85,86] which is then further protonated and ultimately leads to either ethylene or ethanol.[21] After successfully coupling the $*C_1$ intermediates, the reaction must still be appropriately steered to form the correct species to produce the desired C_{2+} product. Ethylene and ethanol have similar pathways and represent the two C_{2+} products that are formed in the highest quantities for almost every catalyst. For most surfaces, ethylene is more easily formed in relation to ethanol, but discussing what aspects enhance ethylene over ethanol becomes much more complicated and cannot be generalized for all catalysts.[5,17,22,87,88] Multiple pathways have been proposed to describe the reaction mechanism after the initial formation of $*C_{2+}$ species, presenting many scenarios that result in poor product distribution. While early pathway bifurcation may allow for the formation of specific C_{2+} products based on only a few reaction steps (**Figure** 3a), it is also possible that the $*C_{2+}$ intermediate is allowed multiple opportunities to alter its reaction path throughout the lengthy reduction process (Figure 3b). CO_2RR pathways that only rely on the formation of a few key intermediates to promote high product selectivity would be most conducive toward allowing for the application of CO_2-to-C_{2+} at an industrial level.

This uncertainty regarding C_{2+} selectivity further convolutes the already complicated mechanism for forming C_{2+} products. It places much more weight on modeling, in situ observation, and applying DFT calculations to better predict and understand the reaction and its products on a given catalyst. Significantly, determining selectivity between different C_{2+} products largely depends on the active site structures,[15,89,90] as well as the dominant $*C_1$ intermediates.[22,91] Precisely determining a singular step that is most important to the selectivity between ethylene and ethanol is highly difficult, mainly because the active site structures within each catalyst can directly affect the mechanism itself. For each catalyst, DFT calculation and in situ observation can elucidate the underlying mechanism taking place, but it is not possible to arrive at a simple answer as to what drives selectivity between C_{2+} products for all catalysts. Overpotential does not seem to have an impact on the selectivity of this process directly due to C_{2+} products having similar equilibrium potentials. However, its role in forming different $*C_1$ intermediates is known, which in turn may have an impact on C_{2+} selectivity depending on the circumstance.[92]

On that note, it is imperative to understand the role that overpotential plays in CO_2RR; many parameters are affected by overpotential. For example, studies have shown that the CO_2RR product distribution of a catalyst is affected by the alteration of the overpotential.[45,86,93,94] Ren et al. showed that lightly reduced C_1 products like CO and $HCOO^-$ are formed at higher rates at potentials above −0.9 V, whereas highly reduced C_1 products like CH_4 are formed at higher rates at potentials below −1.1 V. Meanwhile, in between −1.1 V and −0.9 V, C_{2+} products had a higher formation rate.[93,95] This behavior can be understood by considering the effect of overpotential on reaction rate; the higher the

Table 1. Summarization of the characteristics and components of each of the commonly used electrochemical cells for conducting CO_2RR.

Cell Type	Potential [V vs RHE]	Current Density [mA cm^{-2}]	Details
H-Cell	−0.4 – −1.4 (Cathodic)	10 – 100	Three-electrode system with an anolyte and catholyte separated by an IEM. CO_2 is bubbled and dissolved directly into the catholyte, resulting in low concentration at the catalyst surface. See Figure 4a for a detailed image.
Flow Cell	−0.4 – 1.4 (Cathodic)	50 – 1000	Electrolyte is continuously circulated throughout the cell, with CO_2 being diffused through a GDL at the cathode, enhancing the mass transfer efficiency. See Figure 4b for a detailed image.
Electrolyzer/MEA	3 – 4.5 (Full Cell)	100 – 1000+	A type of Flow Cell that directly interfaces the catalysts with the IEM, thereby eliminating ohmic losses due associated with ion transportation through the electrolyte. See Figure 4c for a detailed image.

potential, the more rapid the reduction of $*C_1$ intermediates. Low potential increases the likelihood of species desorbing from the catalyst surface before undergoing numerous reaction steps, with high potential causing fully reduced CH_4 to desorb. In both examples, a high concentration of mobile $*C_1$ is not maintained, which is required for reliable C_{2+} formation. At middling potentials, the reaction rate occurs at a speed such that $*C_1$ species are maintained on the surface and allowed to move across, introducing the possibility of $*C_1$ interaction and the promotion of the C-C coupling mechanism.

However, the overpotential not only influences the behavior of CO_2RR – the effect of the competing HER must also be considered due to its similar onset potential compared to CO_2RR. Inconveniently, CO_2RR requires the transportation of protons to the catalyst's surface, which makes the progression of HER unavoidable to some extent. A correct cathodic potential should be carefully selected to maximize $*C_1$ intermediate formation and minimize HER. The challenge for researchers attempting to increase performance by inhibiting C_1 and H_2 formation lies in expanding the potential window between these two processes, commonly achieved by reducing the onset potential of CO_2RR or impeding H^+ adsorption to reactive sites.[69,96,97] As discussed previously, a key advantage to producing lightly reduced C_1 products lies in utilizing a less aggressive overpotential, thus preventing the formation of H_2. From an economical perspective, scientists have a vested interest in reducing overpotential so that it is as low as possible. TEAs suggest that a cathodic potential close to −0.7 V versus RHE is a reasonable operating overpotential for profitable CO_2 reduction, and the goal has been met with multiple catalysts.[3,8,14] However, there are additional reasons why lower overpotentials are desirable, such as the mitigation of potential-related degradation mechanisms.[98] Still, the natural behavior of the reaction shows that overpotential has a strong impact on product distribution when conducting CO_2RR,[19,93] not to mention its role in current density.[99] Ideally, new strategies should be developed such that overpotential has a lower influence on the distribution of CO_2RR products. That way the potential can be minimized without requiring a large gap between the $*C_1$ formation onset potential and the C-C coupling onset potential.

Furthermore, overpotential significantly impacts the stability of the catalyst and CO_2RR systems as a whole. Potential-driven catalyst surface reconstruction can be a significant concern from a catalyst perspective. Typically, Cu on these catalysts will dissolve and re-deposit onto another portion of the catalyst, which can be detrimental when these catalysts are so carefully designed to promote a specific reaction pathway.[98,100] Thus, throughout CO_2RR at cathodic potentials, the defect-rich, rough, desirable surfaces will gradually become smooth, reducing the ability of the catalyst to facilitate the C-C coupling step.[101] By limiting the overpotential, the rate at which this occurs can be reduced significantly, resulting in more durable catalysts. However, system stability represents an equally or even more pressing potential-related concern critical for understanding CO_2RR's prospects and challenges as an industrial process, which will be discussed in the following sections.

3. Fundamental Considerations for CO_2RR: A System Perspective

Arguably, the more severe limitation on CO_2RR as an industrial process lies in CO_2RR systems, rather than CO_2RR catalysts. Many factors should be understood from the reactor design perspective. In this section, we will discuss the efficiency of the various electrochemical cells used for CO_2RR and concerns related to system degradation and overall efficacy when examined from an industrial point of view. To accompany this discussion, we have generated a table to briefly describe the operating parameters and characteristics of each electrochemical cell, which may be found in **Table 1**.

3.1. H-Type Electrochemical Cells

The complexity of H-cells is rather low, allowing observers to better understand the catalyst's performance rather than the effect of other factors that may further obfuscate the catalyst's efficiency. H-cells are particularly useful for direct evaluation of the

performance of a catalyst in the laboratory, depicted simply in **Figure 4a**.[99] While there is some variation in the conditions and components used in an H-cell, generally a Pt metal anode performing OER is used as the counter electrode to a given CO_2RR electrode.[102–105] Regarding electrolyte selection, 0.1 M $KHCO_3$ or 1 M KOH are typically used with an ion exchange membrane (IEM), with a reference electrode inserted in the catholyte. The reactor is sealed to ensure the gaseous product is properly collected before being inserted into a gas chromatograph (GC). While in operation, the CO_2 feed is bubbled through the catholyte, which absorbs a small amount of the low-solubility gaseous CO_2 and transports it to the surface of the catalyst, where the reaction proceeds. This method of supplying CO_2 to the catalyst surface is inefficient compared to gas diffusion electrode (GDE) flow cells and reduces the applicability of H-cells. However, thanks to their simplicity, one of their primary uses is as a reactor for catalyst stability tests.[103] Utilizing H-cells for stability testing is prudent for developing a better understanding of the durability of the catalyst directly rather than that of the system in its entirety.

3.2. GDE Flow Cells

Flow cells represent a more industrially applicable cell configuration for high-rate CO_2 conversion, regardless of which product the catalyst is selective for, due to their ability to allow for high CO_2 mass transfer to the catalyst. The key to this enhanced mass transfer lies in the diffusion layer, which acts as a triple-phase boundary (TPB) for gaseous CO_2, aqueous electrolyte, and solid catalyst active sites, bypassing the need to properly dissolve CO_2 into the electrolyte the way an H-cell requires (Figure 4b). GDEs and gas diffusion layers (GDLs) differ in their ability to collect current, causing potential product distribution effects and GDEs are more efficient but more susceptible to electrowetting effects.[106,107] In either case, the layer is hydrophobic and contains a microporous layer onto which a catalyst ink is deposited, which facilitates the formation of the TPB.[108,109] Underneath the microporous layer is a macroporous layer exposed to the gaseous CO_2 feed.

3.3. MEAs and Zero-Gap Electrolyzers

Membrane electrode assemblies (MEAs) have been extensively researched for fuel cell and electrolyzer applications, as they can produce impressively high current densities with low applied potential. The configuration is similar to that of GDE flow cells with the vital difference being that it lacks a liquid electrolyte chamber, instead opting for a humidified CO_2 feed stream (Figure 4c).[110,111] This change reduces the internal resistance of the system by limiting ohmic losses, thus allowing for lower applied potentials overall. As a lab-scale piece of equipment, the MEA suffers due to high complexity and challenging operating condition control, as well as an inability to properly monitor the potential of each electrode due to there being no liquid anolyte or catholyte. Instead, overall cell potential is used to describe these systems, which is not ideal due to the effect of the anodic oxygen evolution reaction (OER). This energy-intensive half-reaction requires significant overpotential.

3.4. Considerations for Flow-Type Cells

In terms of industrial viability, H-cell configurations can be immediately discounted as a possibility due to their highly inefficient CO_2 mass transport properties. This causes a massive difference in current density, showing tens of milliamperes per square centimeter rather than hundreds. Thus, some direct gas diffusion process is required to supply enough CO_2 to the catalyst to obtain sufficient current densities. The capability of these layers can be astonishing with the correct setup, achieving current densities above 1 A cm^{-2} at reasonable overpotentials, easily surpassing the relatively conservative suggestions of many TEAs of ≈300–400 mA cm^{-2}.[3,14,17] Still, high-rate current density is often associated with the deterioration of other vital parameters like selectivity and stability, which can limit the practicality of conducting the reaction in such a high-intensity manner.[16,111,112]

One of the key features that allows for such high current density operation is the gas diffusion layer, which efficiently transports large quantities of CO_2 directly to the catalyst surface. Unfortunately, many flow-cell-specific complications arise from issues with the integrity of the GDL in both GDE flow cells and MEAs. Ideally, the gas chamber should be dry, with no electrolyte bypassing the diffusive layer, a process that is referred to as "flooding".[106] Many conditions can induce this behavior, such as the activity of the GDL itself and, significantly, the overpotential applied to the catalyst.[108] High overpotentials can result in the failure of the GDL, which can be explained by considering the electrowetting effect. This phenomenon causes a change in aqueous surface tension at the surface of a hydrophobic material due to an applied potential.[106,108,113] Electrowetting is unavoidable to a certain extent and disrupts the important TPB necessary for obtaining high-performance CO_2 electrolysis; ideally, there should be a delicate balance of gaseous reactant and liquid electrolyte such that appropriate amounts of CO_2 and protons are supplied to the surface. By adding different dopants to Cu species, the hydrophilicity of the catalyst layer can be augmented to allow for a more hydrophobic interface that is resistant to potential-related electrowetting. However, it has also been found that this changes the selectivity of the catalyst itself, which introduces another layer of complexity to the problem (**Figure 5a**).[114] Alternatively, by operating at a lower potential, the electrowetting intensity will be reduced, providing yet another incentive for scientists to reduce the overpotential to as low as possible. It has been shown that other conditions may influence electrowetting and flooding, such as testing protocols,[106] spontaneous electrolyte organization during the reaction,[5,113,115] or insufficient pressure within the gas chamber.[116] Nevertheless, researchers have recently endeavored to improve these layers with promising results through modifying the system and altering the GDL directly.[117,118] A high-performance 3D-printed polytetrafluoroethylene (PTFE) GDL was printed to allow for careful observation of the effect of CO_2 GDL permeance on the selectivity of a Cu catalyst tested within a flow cell (Figure 5b).[62] The results demonstrate that high CO_2 permeability must be maintained, otherwise the availability of CO_2 on the surface of the catalyst will be low, resulting in a suppressed C-C coupling step and reduced C_{2+} selectivity.

Once flooding begins, the performance of the reaction will be heavily impacted. Notably, the failure of the diffusive layer and the

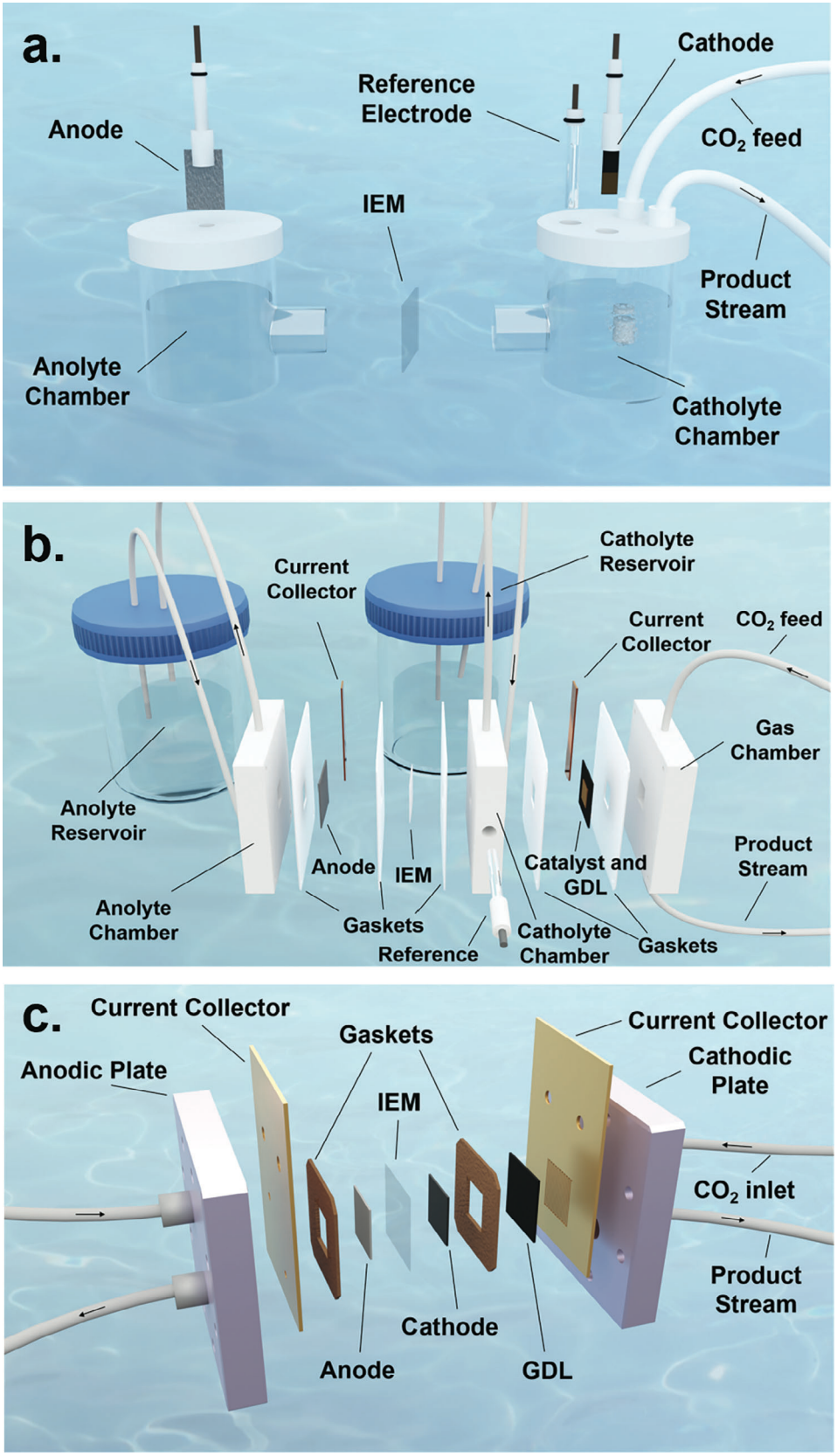

Figure 4. a) Diagram depicting a standard H-Cell for CO_2RR. b) Diagram depicting a standard GDE flow cell for CO_2RR. c) Diagram depicting a standard MEA electrolyzer for CO_2RR.

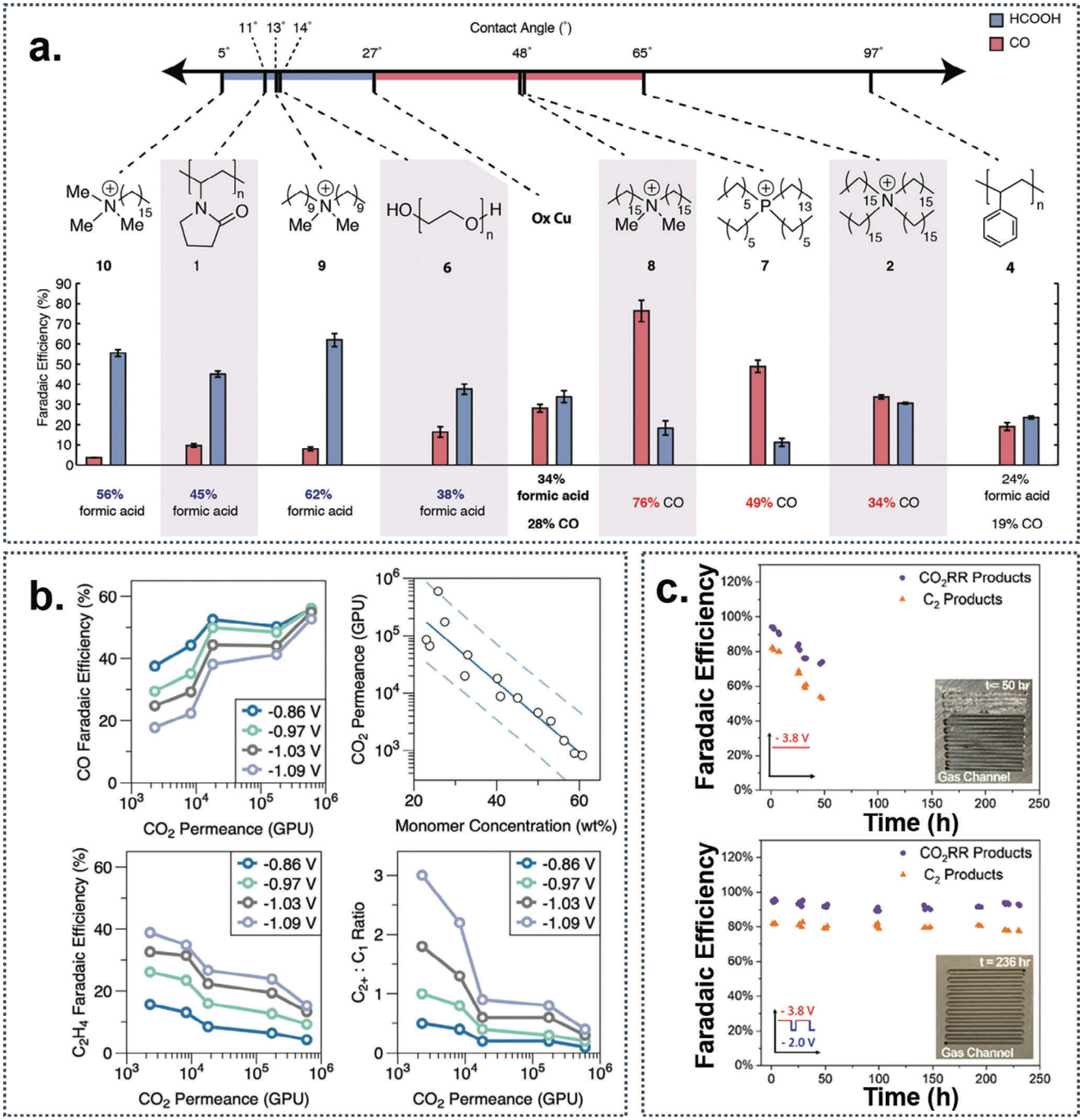

Figure 5. a) Effect of the addition of various organic species on the water contact angle of an oxidized Cu electrode, along with its effect on the FE observed between CO and HCOOH. Reproduced with permission.[114] Copyright 2019, American Chemical Society. b) Effect of CO_2 permeance on the product distribution of a Cu NP catalyst on a 3D printed GDL inside of a flow cell. Reproduced with permission.[62] Copyright 2021, Wiley. c) MEA stability test results obtained for a self-cleaning electrode potential pulsing strategy. Inset images show the state of the gas flow field after testing, which is heavily blocked for non-pulsed operation. Reproduced with permission.[113] Copyright 2019, American Chemical Society.

total coverage of the GDL will force the mass transfer behavior to function more like an H-cell, severely inhibiting CO_2 availability. Droplets may form on the back and inside of the GDL, evaporating and leaving behind salt formed from the electrolyte or solvated CO_2. In either case, these species will effectively disable the reactive sites that impede mass transfer, thereby promoting HER due to a lack of CO_2.[99,119] Counterintuitively, flooding is still possible in MEAs despite only using a humidified CO_2 feed stream, since bicarbonate salt is formed as CO_2 interacts with the water in the stream, which may then be deposited within the MEA flow field, blocking sites and causing system failure.[4,107,111] Careful relative humidity (RH) selection is necessary to reduce

the likelihood of this process.[111] Simultaneously, other types of GDL failure can cause significantly different behavior within CO_2RR, such as cracking, which lowers the ability of the GDL to properly interface with the catalyst.[119] Other solutions hold promise, such as the development of augmented system operation strategies such as Xu et al.'s "self-cleaning" strategy that utilizes cyclic potential application to regenerate activity losses, leading to much higher stability (Figure 5c).[113] In essence, the technique inhibits the precipitation of salts within the gas flow channels, resulting in much higher system stability. Ultimately, this process can be controlled in many ways within MEAs and flow cells. The challenge lies in the transfer of excessive anions across the IEM, which increases the concentration of the catholyte side of the reactor. Once this reaches a certain point, anion or bicarbonate salts will precipitate onto the catalyst layer, blocking active sites and reducing performance, and causing the CO_2 absorbed into the electrolyte to be wasted. Thus, by introducing new ways to control the ion concentration in the catholyte, the systemic stability of the cell can be enhanced. Some of these techniques are very simple, such as periodically rinsing the cell with water to remove excess anion crossover, that prevent the transfer of large K^+ ions at the expense of reduced permeability (**Figure 6a**).[120]

By its nature, the CO_2 crossover concern is only a major issue with anion exchange membranes (AEMs), since CO_2 crossover depends on the transfer of anionic CO_32^- ions across the membrane. Thus, other types of IEMs like proton exchange membranes (PEMs) or bipolar membranes (BPMs) may be utilized to effectively suppress enhance CO_2 feed utilization. Diagrams depicting an AEM, PEM, and BPM may be found in Figure 6b. Nevertheless, these options do come with challenges that decrease their attractiveness when compared with AEMs. For the usage of PEMs, the CO_2RR catalyst must have the ability to efficiently suppress the progression of HER, which becomes dominant in acidic conditions. Thus, the discussion pertaining to the application of PEMs for CO_2RR electrolyzers will be carried out in Section 5.4.3. Alternatively, BPMs have issues relating to energy efficiency due to the inclusion of an internal catalyst that splits water into H^+ and OH^-, allowing for a net ion transport across the membrane. As such, efforts to improve the performance of AEMs have become a focus of researchers aiming to mitigate CO_2 crossover as well as salt deposition.[121] AEMs can be customized through the usage of different functional groups that show an ability to reduce the movement of CO_2 across the membrane. For example, it has been found that quaternary ammonium poly(*N*-methyl-piperidine-co-*p*-terphenyl) exhibits higher selectivity, ion conductivity, and stability when compared to the imidazolium-functionalized poly(styrene) background present in Sustainion.[112,122,123] The development of new AEM materials may result in reduced CO_2 crossover and higher efficiency, especially with materials that show reduced water uptake, thereby inhibiting anion conductivity.[124] Unfortunately, the reduction of anion conductivity simultaneously reduces the conductivity of both the unwanted species as well as the ideal OH^- ion transport, since this method relies on increasing the overall mass transfer resistance of the membrane.[112,125] Further, while some research has been conducted on increasing the membrane selectivity of AEMs within artificial photosynthesis,[124,125] the elevated potentials required to drive CO_2RR promote the transfer of unwanted species, especially at high current and low flowrate.[126] In addition of the transfer of CO_3^{2-}, collecting liquid products can be severely complicated when the membrane is vulnerable to ion crossover, since desirable species like formate and acetate are very susceptible to crossover processes.[126] Similarly, neutral species like alcohols can also migrate across the membrane as well, but at a reduced rate.[127,128] Thus, the promise of BPMs for CO_2RR has increased in recent years, particularly for C_{2+} selective processes, which can lose the majority of fed CO_2 due to electrolyte crossover.

As such, the usage of BPMs as a method for improving the SPC of CO_2 electrolyzers also has promise. Functionally, BPMs work differently from PEMs and AEMs in that the layer is formed by combining the two.[131,132] Instead of permitting penetration through the entire membrane, BPMs prevent the full transport of ions through the layer, further inhibiting the interaction of the anolyte and catholyte. This increases the resistance of the layer, but also all but removes CO_2 crossover as a significant challenge for electrolyzers conducting CO_2RR.[4,18,133] Still, promising energy efficiency can be obtained by operating the electrolyzer in such a way that works with the strengths of the BPM.[130,134] It was found that the CO_32^- stored in the electrolyte can be released and utilized at the cathode by modifying the electrolyte and reducing the CO_2 flowrate while taking advantage of the impermeability of the BPM (Figure 6c).[129] Thus, by harnessing the stored CO_32^- the SPC may be improved to much more industrially viable levels. Alternatively, there have been recent results that indicate that the usage of both a PEM and an AEM can operate in tandem to allow for efficient CO_2 crossover suppression and extended stability while maintaining competitive current density and FE (Figure 6d).[135] The researchers found that $FE_{ethylene}$ was improved slightly in comparison to an electrolyzer with an AEM, but the selectivity of ethanol was greatly enhanced, perhaps due to liquid product crossover complications with the AEM.[126,130]

Within MEAs, an extra concern related to the deposition of the catalyst layer is introduced. Since MEAs do not have a liquid electrolyte, the anode and cathode catalyst layers are placed directly on a solid polymer electrolyte membrane. MEAs typically contain specifically proton exchange membranes (PEMs) that are not conducive for CO_2RR since PEMs transfer positively charged protons that reduce the pH of the PEM (and catalyst) surface. With lower pH, suppressing HER progression becomes much more difficult, not to mention the absence of positive Helmholtz layer intermediate interactions observed in high-pH reaction environments.[112,136] Nevertheless, researchers have begun devoting efforts to realizing neutral and acidic condition CO_2 electroconversion, increasing the viability of MEAs for CO_2RR.[137,138] Alternatively, modified GDE flow cells containing a thin catholyte layer have been explored to reduce the ohmic resistance without necessitating full transition to MEA operation.[16]

MEA electrolyzers will certainly be the most optimal reactor for conducting CO_2RR at industrial scales in the future, but new strategies for inhibiting MEA-specific problems are required to enable their full potential. Beyond flooding, other issues can introduce over- and underestimations of the catalyst performance, such as not measuring the flow rate leaving the cell,[4] incorrect or absent iR compensation usage,[139] incorrect GC or high-performance liquid chromatography (HPLC) calibration,[40] poor control of the pH and/or electrolyte inside of the flow cell,[140] bubble formation on the surface of the catalyst,[106] or electrolyte

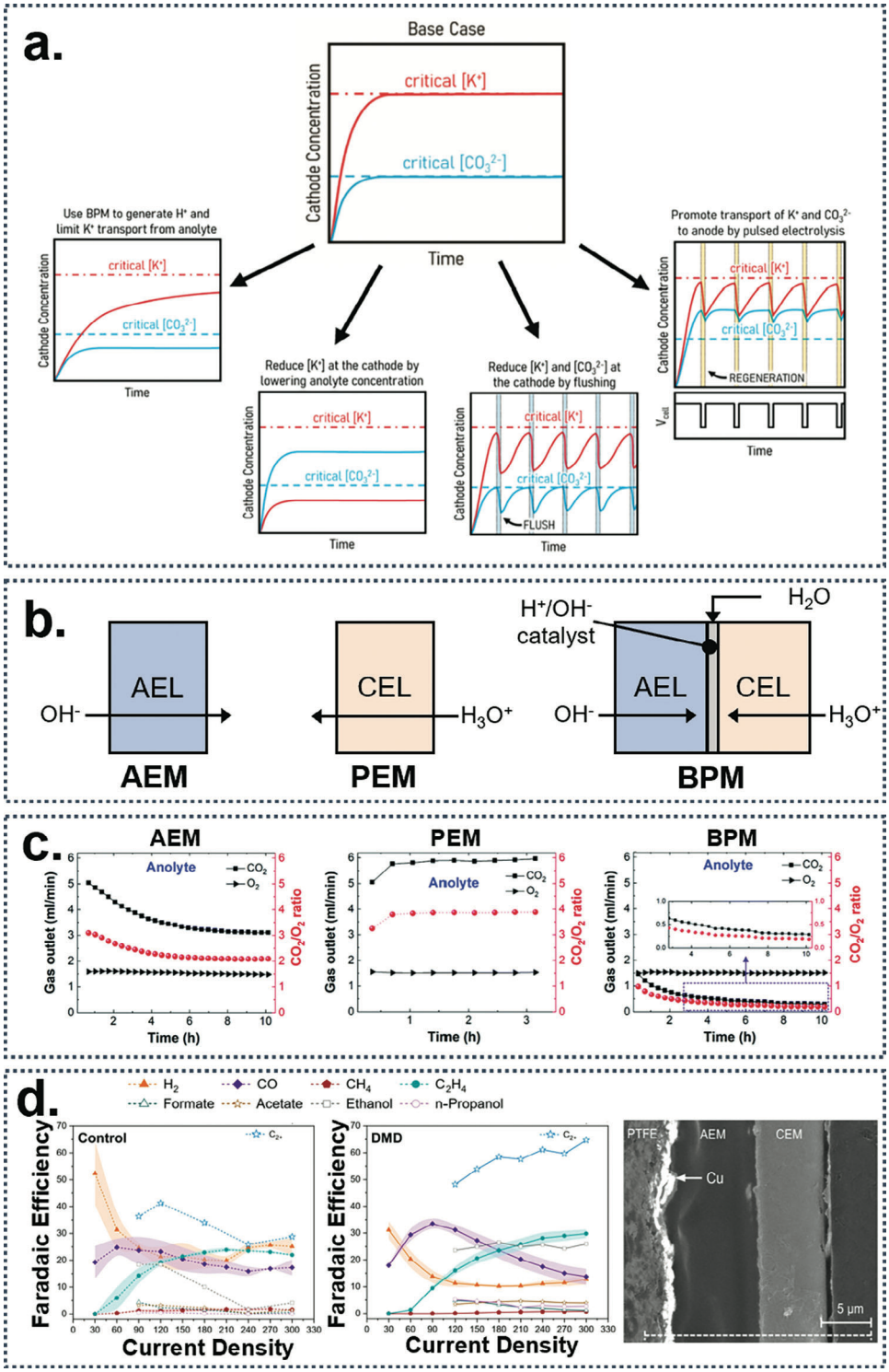

Figure 6. a) Four proposed strategies for controlling the precipitation of anion salts within MEAs for CO_2RR. Reproduced with permission.[120] Copyright 2023, American Chemical Society. b) Simplified diagrams for the function of anion exchange membranes (left), proton/cation exchange membranes (middle), and bipolar membranes (right). c) Comparison of the ratio of CO_2/O_2 in the anode gas outlet between electrochemical cells using an AEM (left), PEM (middle), and a BPM (right). Reproduced with permission.[129] Copyright 2020, Royal Society of Chemistry. d) Left: current density and FE data for an MEA electrolyzer utilizing an AEM; Middle: current density and FE data for an MEA electrolyzer utilizing a 1:1 AEM:CEM MEA; Right: cross-sectional image of the 1:1 AEM:CEM MEA developed by Alkayyali et al. Reproduced with permission.[130] Copyright 2023, American Chemical Society.

crossover through the IEM.[111,112] CO_2RR-to-C_{2+} processes are highly complex, and poor maintenance of the TPB further exacerbates any problems that may be encountered. Therefore, researchers must verify that their equipment functions correctly and that all extraneous effects are compensated for.

Perhaps due to how unforgiving the reactor is, stability is the least studied characteristic of electrocatalytic systems for CO_2RR. While other performance metrics continue to advance, stability is often only tested on the scale of tens to hundreds of hours.[15,103] Neither of these results compare favorably with the lifetimes suggested by TEAs, which range significantly between 20 000 and 80 000 h in either GDE flow cells or MEAs.[14,17,40] It is of critical importance that the stabilities of these systems are not neglected as the other metrics approach their performance goals. Unfortunately, conducting stability tests on the scale of thousands or tens of thousands of hours is costly and certainly time-consuming. However, increasing the stability of a CO_2RR system should be viewed in a more holistic sense, which is to say that purely focusing on the catalyst stability will not necessarily make a catalyst more viable industrially since other detrimental system degradation mechanisms have not been addressed. Despite their differences, lessons can be taken from other electrocatalytic reactions, like the ORR.[141] By analyzing and adapting the techniques previously developed by these researchers, the stability of CO_2RR systems could be enhanced. For example, the development of standardized procedures like accelerated stability testing (AST) to rapidly evaluate the longevity of ORR catalysts helped to alleviate the problem of time-consuming stability tests, for which CO_2RR does not have an equivalent protocol. On the other hand, CO_2-to-C_{2+} electroconversion has many more steps than ORR, meaning that simply cycling the potential may not be enough to capture the degradation behavior. Further, the potential range that ORR typically operates at is higher than that of CO_2RR, meaning that the relevant degradation mechanisms for each system could be different.

Systems like ORR, however, cannot help in solving other grand challenges faced by CO_2RR. While CO_2 crossover during ORR represents a fundamental challenge in practical MEA application, CO_2 presence in the electrolyte of CO_2RR systems is required.[142,143] Particularly for CO_2RR systems with low overpotential, the sources of instability often originate from the reaction environment, not the catalyst itself.[144] The optimization of alternative cell orientations,[26] improved IEMs,[112] novel strategies to regulate the organization of electrolytes,[113] and enhanced GDLs will undoubtedly be more influential on the lifetime of industrially applicable CO_2RR cells.[107] Another route toward achieving industrial viability for CO_2RR in MEAs is to improve the performance of the anode.[111] Typically, a precious metal catalyst conducting OER is used as the counter electrode in these systems, which is relatively sluggish and has a high energy requirement.[145,146] As the OER performance improves, the applicability of CO_2RR will also improve; alternatively, platinum-group metal (PGM)-free OER catalysts could be included instead of the current costly Ir and Ru-based materials.[147]

4. Economic Efficiency of Ethylene Electrosynthesis

Ethylene itself possesses a key role in the current economy as a precursor for creating valuable plastics, like polyethylene and poly(vinyl chloride), or solvents like ethylene glycol. Typically, the ethylene being utilized in these processes comes from environmentally-unfriendly processes like steam cracking of natural gas, thereby emitting large amounts of CO_2 into the atmosphere.[148,149] Unfortunately, polyethylene in particular is nearly unavoidable in modern life, and no suitable replacements have been found that have the same desirable properties with fewer associated environmental concerns. Thus, CO_2RR can provide a pathway toward taking advantage of CO_2 flue gases to synthesize ethylene cleanly.[150] Other methods of producing ethylene cleanly exist, such as biological production of ethylene, which requires biomass as a source of energy.[151,152] Meanwhile, an electrochemical approach benefits from a more easily integrated reliance on electricity, which is more easily accessible than large quantities of biomass.[153]

A simplified, typical CO_2RR system aiming to produce ethylene has been depicted in **Figure 7a**. The baseline steps within an industrially compatible CO_2 electroconversion system are consistent across multiple products, as fundamentally many of the processes required are similar to each other. For example, in-plant harvesting of CO_2 from the flue gas is typically conducted with ethanolamine chemical adsorption. This represents a significant cost for these types of systems due to CO_2 capture inefficiency, typically ranging from \$50–\$70 per ton of CO_2 harvested from a typical flue gas.[14,18] Additionally, certain gas separation protocols must be present in each CO_2RR system, such as purified CO_2 recycles and CO/CO_2 separation.[153] Depending on the type of cell being utilized,[154] anodic counter reaction,[40,155] pH conditions,[154] and membrane being used,[130,134] CO_2/O_2 gas separation of the anode outlet may also be necessary. Simply improving these aspects of a possible CO_2 conversion strategy would improve the viability of all CO_2RR products, not just ethylene.

On this note, however, it is important to acknowledge the role that the counter electrode plays within the economics of CO_2RR implementation. Through the use of OER, O_2 may be obtained along with the CO_2-derived products from CO_2RR, which plays a crucial role in the profitability of these systems.[156] Nevertheless, this process is often severely impacted within traditional CO_2RR electroyzers due to the crossover of CO_2 from the catholyte to anolyte, which results in CO_2 contamination in the anodic gas stream.[112] Naturally, this necessitates additional cost-intensive separation processes to purify the O_2 stream.[153] One solution to this problem is the utilization of a different anodic reaction that does not suffer the same inefficiency as the OER.[26,157] Based on the technoeconomic analysis conducted by Na et al., Organic Oxidation Reactions (OORs) may possess some promise for producing high value anodic products without the need for O_2-CO_2 separation (Figure 7b).[40,155,158]

Ethylene compares favorably to heavily reduced C_1 products like methane and methanol, mainly due to the large market for ethylene as well as the low efficiency of methane and methanol.[18] C_{2+} products and heavily reduced C_1 products share similar efficiencies as compared to lightly reduced C_1 products, since while they are chemically different, they are the same in terms of the challenges that they face.[5] Both of these classes of product typically have reduced FE, higher kinetic overpotential requirement, and have extended reaction mechanisms that involve more electron transfer steps, reducing the quantity of

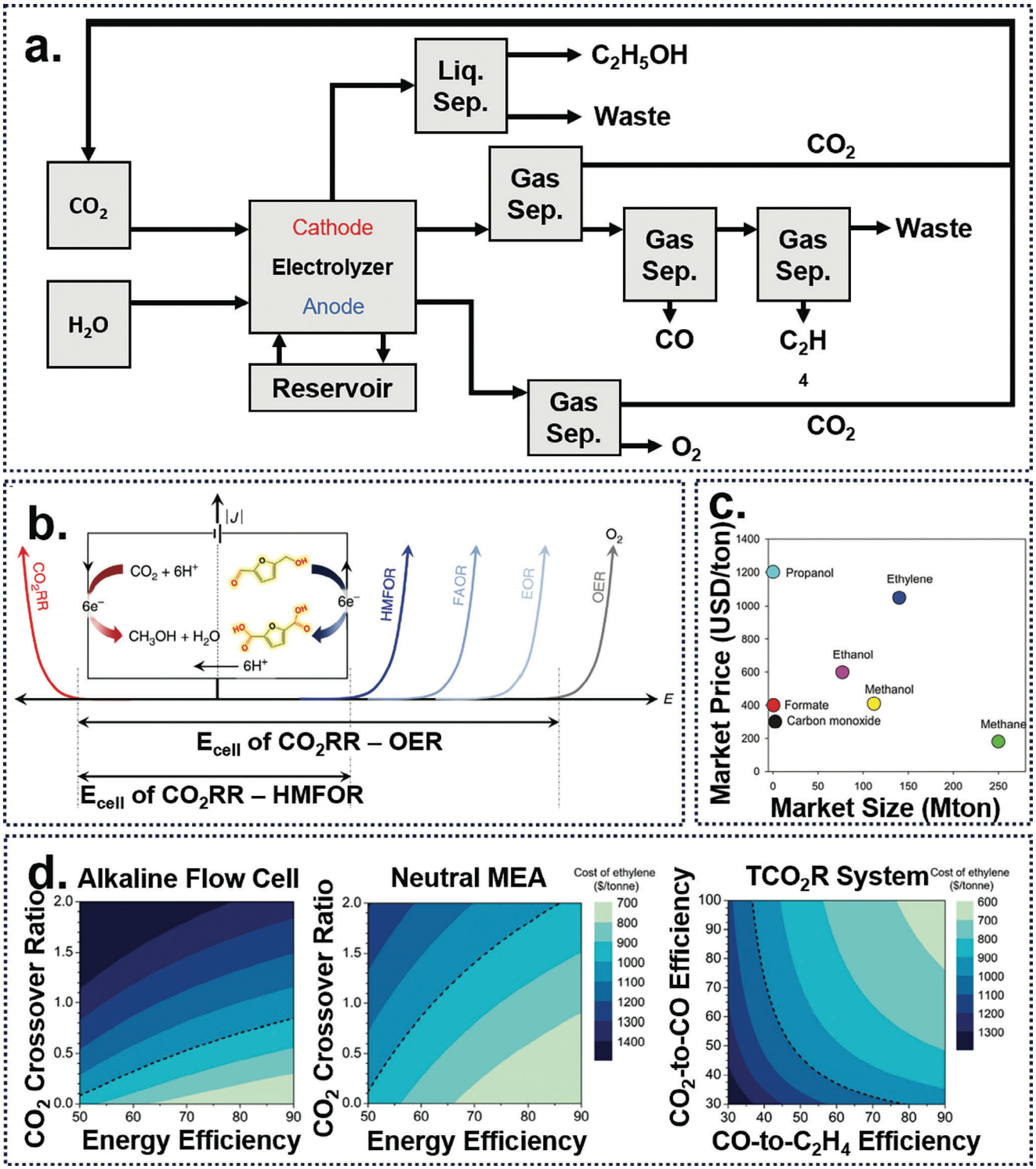

Figure 7. a) Simplified example of an industrial ethylene electrolyzer setup. b) Schematic describing Na et al.'s modeled system, which uses HMFOR rather than OER for reduced CO_2 crossover, lower potential, and more valuable anodic product. Reproduced with permission.[40] Copyright 2019, Nature Portfolio. c) Market price and size comparison of the most common CO_2RR products. Reproduced with permission.[18] Copyright 2019, Wiley. d) Left: comparison of the CO_2 crossover and the electrical energy efficiency of an alkaline flow cell and a neutral-pH MEA. Right: C_2H_4 production cost associated with the Tandem CO_2R electrolyzer system described within Sisler et al.'s technoeconomic analysis. Reproduced with permission.[162] Copyright 2021, American Chemical Society.

product obtained in relation to the current density.[8,159] Further, these products require more separations in total due to the presence of a higher quantity of species in the product stream, since lightly reduced C_1 products like CO may only have CO_2, CO, and H_2 in the outlet mixture. While these characteristics impede methane and methanol,[14,160,161] the improved market value of ethylene allows it to remain an enticing product.

Among multi-carbon products, ethylene is currently the most promising species to produce due to the natural inclination of Cu surfaces. As such, while ethanol is a highly desirable product with a multitude of usages, the selective production of ethanol has proven to be quite difficult for the time being. Another key benefit of producing ethylene is it has much simpler and cheaper downstream processes, owing to its naturally gaseous state.[17,18] To exacerbate this issue, liquid C_{2+} products may also be lost to product evaporation out the back of the GDL, transporting a portion of the liquid species to the wrong separation process.[126,127] A number of high-efficiency gas separation processes have been shown to have good compatibility with the distribution of CO_2-to-C_2H_4 product streams.[18,153] Thanks to all of these characteristics, multiple propositions have been made showing that environmentally friendly solutions are competitive with the current techniques for producing ethylene.[153,163] Notably, the Sargent and Sinton groups have done much work on developing practical industrial strategies for improving CO_2RR viability as well as critically evaluating the efficacy of these approaches. For example, Alerte et al. recently released a TEA showcasing reasonable conditions toward realizing a profitable ethylene production strategy through a more traditional approach.[153]

When compared to CO_2-to-CO conversion, electrosynthesis of ethylene has a number of deficiencies that hinder its applicability. The first of the two challenges that CO_2-to-C_2H_4 conversion faces is unfavorable reaction characteristics when compared to CO_2-to-CO.[14,164] Facilitating high FE for CO has mostly become trivial due to the material characteristics of the catalysts being used. With >95% FE_{CO} having been achieved with such ease thanks to the simple reaction mechanism,[47,48] researchers have devoted more time into developing the other important characteristics for industrial applicability, such as encouraging high stability and current density.[122,165,166] Beyond that, there has been more focus on adapting CO-selective CO_2RR to acidic conditions, which can further improve CO_2 utilization and efficiency within industrial contexts.[138,167] In contrast, much of the work devoted toward the production of ethylene has been aimed toward improving the $FE_{ethylene}$ of the catalyst.[41] For years, the development of a generalizable model of the reaction mechanism has eluded researchers due to the plethora of thermodynamically plausible reaction pathways and intermediates. Nevertheless, promising work has demonstrated the potential that CO_2-to-C_2H_4 conversion possesses within industrial settings. High current density and stability have been achieved multiple times through catalyst innovation and system design ingenuity.[16,54,74,82,113,135,168,169] Meanwhile, valuable insights into the governing principles behind high $FE_{ethylene}$ continue to be published, further advancing the field toward higher selectivity.[80,81]

The second challenge faced by industrial ethylene electrosynthesis relates to more complicated downstream separation processes. Yet another boon for CO production lies in its narrow product distribution, which will often only show CO and CO_2, with trace amounts of H_2 as measurable gaseous species in the outlet.[14,156] Meanwhile, the synthesis of ethylene will not only contain all of the contents of CO_2-to-CO systems, but also C_2H_4, higher amounts of H_2, and trace amounts of CH_4.[162] Typically, pressure-swing adsorption (PSA) is used for this gas separation process since it has relatively high efficiency for separating products of this class.[17,18] On the other hand, the challenge is even more apparent for liquid species – while CO-selective systems may only contain HCOOH, due to poor selectivity between C_{2+} products there will likely be C_2H_5OH, n-C_3H_7OH, i-C_3H_7OH, CH_3COOH, CH_3OH, among other trace species present in the liquid product profile.[18,40] While the separation of so many species is challenging, HCOOH as a primary product also faces challenges within CO_2RR due to the similarity between the boiling temperature between HCOOH and water.[14,164] On the surface, one may not expect this inefficiency to be particularly relevant to ethylene-selective CO_2RR. Nevertheless, the excess C_{2+} products left in the electrolyte do possess high market value and contribute to the overall economic feasibility of the process.[17,161,164] Thus, depending on the concentration of the species in the electrolyte, it may be crucial for the products to undergo distillation. Naturally, as the understanding of what drives selectivity between C_{2+} products, CO_2RR catalysts should have more control, reducing the need for such extensive separation.

In isolation, these problems may not be much of an issue since the ethylene market has advantages over the CO market, primarily due to the relative size of the ethylene market compared to that of CO,[18,170] as well as the increased price per ton of ethylene.[18,162] Unavoidably, the CO_2-to-C_2H_4 requires 6 times more electron transfer steps, significantly reducing the ethylene yield and meaning that on a molar basis, the amount of ethylene obtained will be smaller than what would be produced had the electrons been used to produce CO. Nevertheless, the desirable market is the factor that supports ethylene production the most. Put together, they represent a grand challenge for the industrialization of ethylene that must be diligently worked on to improve CO_2-to-C_2H_4 viability. CO_2-to-C_2H_4 conversion shows significant promise when compared to traditional steam cracking methods, which is enough to justify its application within industrial settings.[163]

To better illustrate the value of ethylene, one should consider that while CO_2RR is nearly ready to comfortably replace other means of CO production, the market is limited at a size of 3–4 billion USD.[170] Thus, it would only be a reasonable method for mitigating a small amount of the pollution produced by industrial processes before the market is oversaturated. In contrast, ethylene represents an in-demand, vital chemical that is a key component for the production of plastics. As such, estimates of the ethylene market size range from 150 to 250 billion USD,[170] with hundreds of millions of tons of ethylene produced annually (Figure 7c).[18,153,162,171] Thinking beyond the appeal of just ethylene as a primary product, from a research perspective there is only a limited amount of knowledge that can be transferred to C_{2+} optimization from such simple C_1 product systems like CO- and HCOOH-selective CO_2RR. Meanwhile, the governing principles of C_{2+} systems are constant between each version of CO_2RR, ensuring that by developing ethylene-selective CO_2RR other C_{2+} reactions are elevated as well.[5] So, although ethylene represents the most promising C_{2+} product,

other high market value C_{2+} species are merely held back by lackluster performance.[14,17] Through the advancement of efficient, economical, environmentally-friendly ethylene electrosynthesis via CO_2RR, more knowledge is gained that could propel ethanol or propanol to the forefront as attractive products. Therefore, although CO_2-to-C_2H_4 electroconversion displays ample pitfalls and hurdles to overcome, it is still of critical importance for the realization of a sustainable global carbon economy using new strategies and approaches to catalyst design and system design.

To this end, the usage of two electrochemical systems operating in tandem has shown promise, whereby CO_2-to-CO electroconversion is performed first before CO-to-C_2H_4 electroconversion is utilized.[154,171,172] The principles behind the catalyst design are mostly the same, as the most important characteristic in both circumstances is facilitation of high *CO surface concentration and efficient C-C coupling active centers. By utilizing this two-step system however, energy requirements may be reduced. Further, CO_2 throughput may be enhanced greatly as well, since the single-pass conversion (SPC) efficiency of CO_2-to-CO and CO-to-C_2H_4 are both higher than the SPC of a traditional CO_2-to-C_2H_4 system. Additionally, CO production within CO_2-to-C_2H_4 systems represents an incredibly common source of reduced FE, which is no longer a concern within CORR systems. Perhaps the most exciting aspect of this tandem process is the possibility to prevent CO_2 loss as CO_32^-, which poses a number of issues like flooding behavior and loss of reactant.[159,162] Since the environments can be tuned separately, the process can be designed such that a solid oxide electrochemical cell (SOEC) is used for the CO_2-to-CO step, which completely removes the possibility of the formation of CO_32^-.[173,174] Subsequently, the pure CO product stream being fed to the alkaline cell conducting CORR is unable to form CO_3^{2-} in the electrolyte, which can drastically reduce the costs associated with regenerating the electrolyte by recovering the excess CO_3^{2-} (Figure 7d).[162] Logistically, this approach suffers from a much more complicated setup, since two cells must be used with different conditions.[175] Intuitively, more separation processes and recycle streams are necessary to ensure the CO_2 is not being fed into the cell conducting CORR.[172] Other novel strategies such as the implementation of a two-layer electrode with differing catalysts, one for CO_2-to-CO and one for CO-to-C_2H_4, showed much improved FE, current density, and SPC in relation to a traditional Cu-based CO_2RR catalyst.[168] In particular, by layering a highly CO-selective CoPc-based material over a traditional polycrystalline Cu catalyst, the system was able to provide adequate performance inside of an acidic electrolyte. Changing the membrane being used also shows significant promise for lowering the cost per ton of ethylene through the prevention of CO_2 crossover and extension of stability, whether it involves the usage of a BPM or another novel strategy.[131,134,135]

5. Effective Strategies for Ethylene-Selective Electrocatalysts

5.1. Multicomponent Catalysts

5.1.1. Multimetallic Catalysts

Multimetallic CO_2RR catalysts utilize multiple metals to raise the activity of the Cu active sites, usually by metal-metal interactions involving the reorganization of electrons and the creation of a local environment conducive to adsorbing and catalyzing fed CO_2.[176] Conversely, these additional metals may be used to promote secondary active sites that help facilitate different stages of the reaction. Over the years, multimetallic catalysts have been researched heavily due to the utility posed by alloys and other multimetallic materials for enhancing intrinsic activity.[177] In terms of CO_2RR, alloys have been historically more effective for forming products other than ethylene, whereas ethylene has benefited more from modified Cu surfaces. Nevertheless, high performance has been found with a CuAg alloy nanowire catalyst produced by Hoang et al., from which the researchers were able to determine the existence of a synergistic Cu-Ag interaction due to the formation of $*C_1$ intermediates at Ag sites.[76] Alternatively, Xiong et al. synthesized well-defined Ag-Au cubic nanoframes as a host for Cu, which boasted ≈77% $FE_{ethylene}$ within a flow cell (**Figure 8a**).[178] In this case, the utilization of a heterometallic support enabled the formation of a well-controlled catalyst morphology, while also taking advantage of altered catalytic properties based on metal-metal interactions. Similarly, Koolen et al. have developed a fundamentals-driven material design approach toward creating differently nanostructured Cu- and CuAg-based catalysts, demonstrating adjusted selectivity for each (Figure 8b).[179] Notably, while the overall C_{2+} FE and HER inhibition of the nanostructured CuAg catalysts improved, selectivity for ethylene in relation to other C_{2+} products was decreased. Jiang et al. recently observed interesting behavior from their Ag nanoparticles on Cu nanowires catalyst, exhibiting good ethylene formation in an alkaline zero-gap electrolyzer.[180] Still, high performance was obtained using a $Cu_{10}La_{0.16}Cs_{0.14}$ catalyst, which obtained 70.5% FE for C_{2+} products in a flow cell (Figure 8c).[181] In each of these cases, it was understood that adding additional metal species altered the electronic structure of Cu or participated in the reaction directly to increase the selectivity of the catalyst for CO_2RR toward C_{2+} products. As mentioned, other alloy catalysts have been investigated for ethylene production, such as CuAu,[182] CuSb,[183] CuZn,[184,185] CuCo,[186] CuHg[187] CuPd,[84,188] and others,[80–82,181,187,189] typically showing good C_{2+} performance but relatively low selectivity for a single C_{2+} product.

In essence, the inclusion of additional metals to these catalysts strongly impacts their adsorption and reactive properties, particularly for alloyed catalysts. As such, it is often found that non-Cu monometallic catalysts have undesirable product distributions when optimizing for C_{2+} formation due to large amounts of C_1 products. Metals like Ag, Au, Sn, and Fe have all been shown to be active for highly reduced C_1 formation due to their much stronger binding of adsorbed C_1 species that holds them more aggressively to the active sites, preventing them from transporting across the surface and producing C_{2+} species.[83,193] From a different perspective, Ni has also been shown to be selective for 2-electron reduced CO due to its weak carbon dioxide adsorption.[194] Combining these metals with Cu makes it possible to modulate the adsorption strength of the reactive surface, thereby altering the favorable reaction pathways. Kim et al. have recently developed a comprehensive study on the fabrication of Cu alloy materials that can control the selectivity of either ethylene or ethanol using a non-equilibrated method (Figure 8d).[190] One of the key factors that

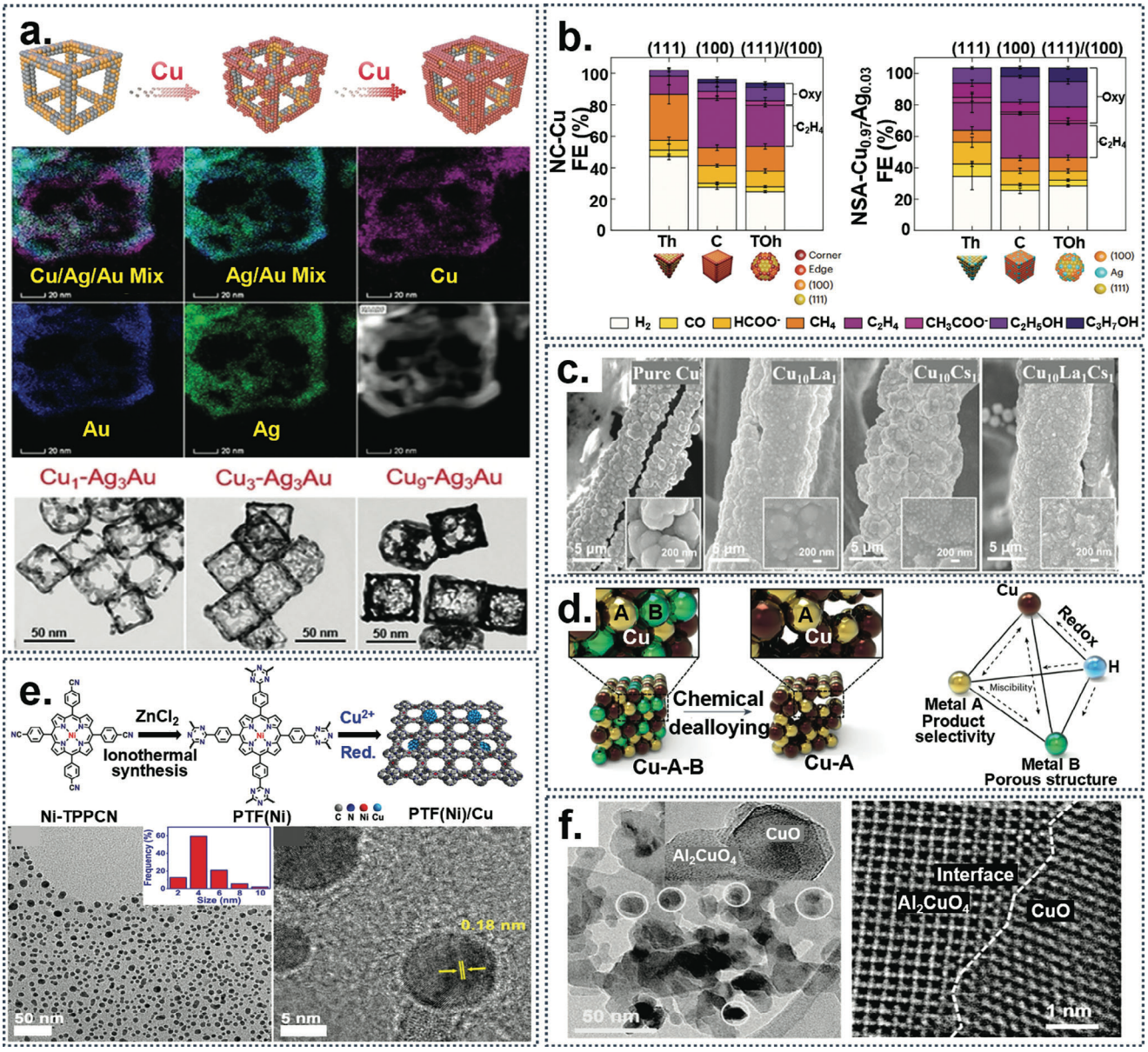

Figure 8. a) Design of Xiong et al.'s Cu-based AgAu nanoframe catalyst. Top: schematic illustrating the deposition of Cu onto the AgAu cubic nanoframes. Middle: TEM images showing the elemental distribution of the Cu-AgAu nanoframe catalyst using EDX. Bottom: HRTEM images showing the morphology of the Cu-AgAu nanoframe catalyst with different Cu loading. Reproduced with permission.[178] Copyright 2020, Wiley. b) FE data acquired from various Cu- and CuAg-based nanostructured catalysts. Reproduced with permission.[179] Copyright 2023, Springer Nature. c) SEM images showing the structure of the Cu-based multimetallic catalysts produced by Jia et al.[181] d) Diagram depicting the general strategy for controlling the product distribution of Cu-based catalysts using alloy materials. Reproduced with permission.[190] Copyright 2023, Springer Nature. e) Meng et al.'s Cu NPs @ Ni-N-C tandem catalyst. Top: schematic diagram detailing the synthesis. Middle: TEM (left) and HRTEM (right) of the Cu NPs @ Ni-N-C catalyst, showing good nanoparticle dispersion. Bottom: EDX analysis via HRTEM showing the elemental distribution of the Cu NPs @ Ni-N-C catalyst. Reproduced with permission.[191] Copyright 2021, Wiley. f) Electron microscopy images of the CuO/Al_2CuO_4 catalyst produced by Sultan et al. Left: TEM images showing the separation of CuO NPs within the Al_2CuO_4 structure. Right: STEM images depicting the boundary between CuO NPs and the Al_2CuO_4 domain. Reproduced with permission.[15] Copyright 2022, Royal Society of Chemistry.

negatively impacts alloys of this nature is the continuous reactive surface. Functionally, maintaining a high enough $*C_1$ concentration across the entire catalyst surface to enable competitive C_{2+} formation is not especially feasible. Still, by manipulating the adsorption properties of the surface, it is possible to create regions of high $*C_1$ concentration at locations that facilitate C-C coupling. This approach is commonly referred to as "tandem" catalysis, by which two species synergistically work together to direct product distribution, as illustrated by Meng et al.'s work creating Cu nanoparticles (NPs) anchored on a Ni-N-C support (Figure 8e).[191,192,195] From a mechanistic perspective, this approach aligns closely with the

general understanding of CO_2RR itself. Intuitively, a catalyst must use a two-step process to transform CO_2 to C_{2+}, which naturally suggests the combination of two catalytic surfaces or reactive sites.

To illustrate this effect, Sultan et al. synthesized a CuO/Al_2CuO_4 catalyst that showed high performance for ethylene, achieving an ethylene FE of 82.4% in an H-cell, which was mostly stable for 100 h, as well as a $FE_{ethylene}$ of 70% in a flow cell with 600 mA cm^{-2} (Figure 8f).[15] In situ data showed the ability of the catalyst to continuously maintain high concentrations of *CO species in relation to the CuO control sample, leading to a high rate of C-C coupling and ethylene formation. Mechanistically, they determined that the CuO surface could selectively produce CO, which was then desorbed and re-adsorbed into the Al_2CuO_4 surface that promotes the C-C coupling step and subsequent ethylene formation. Efficient tandem catalysts for CO_2RR directly allow the transport of the $*C_1$ intermediates to the sites that couple them. Thus, an effective method for fostering this exchange is reducing the distance between the reactive sites. For phase-segregated morphologies this represents a fundamental challenge due to the difficulty of dispersing the reactive sites thoroughly, which is contrasted by other methods of incorporating multiple active sites in a catalyst, namely via defect introduction or nanostructuring.[69,105,196] While many exciting combinations and morphologies have been developed, for this reason many phase-segregated catalysts face challenges in obtaining the same performance as other varieties.[68,191]

5.1.2. Metal-Nonmetal Catalysts

Similar to multi-metallic catalysts, metal-nonmetal catalysts can be formed to increase the activity of the active material.[61] With the exception of oxides, metal-nonmetal catalysts have been relatively under-researched despite impressive performance, particularly for halogen-modified Cu.[197] Ma et al. reported a fluorine-modified copper sample that displayed a fantastic current density of 1.6 A cm^{-2}, with an impressive overpotential of only −0.89 V versus reversible hydrogen electrode (RHE) and a C_{2+} FE of 80% (65% ethylene, 15% ethanol).[54] They concluded that the reason for this enhanced performance is the way that fluorine promotes H_2O dissociation to increase the *H particles present to enable the hydrogenation of intermediates while suppressing HER, which has been observed by other researchers as well (**Figure 9a,b**).[54,198] Interestingly, DFT calculations suggest that the thermodynamically favorable formation of *OCHCHO is dominant and dramatically enhanced, to the point that $*C_1$ intermediate formation is actually the rate-limiting step.

In contrast, Li et al. published a Cu/CuI catalyst that showed good performance: 71% FE for C_{2+} products with 894 mA cm^{-2} at −1.0 V that is stable for 85 h, fabricated by the physical mixing of powdered precursors.[199] The iodine content in the CuI regions is removed from the surface during the reaction, forming a nanoporous Cu_2O morphology that helps to catalyze the coupling reaction (Figure 9c). Meanwhile, Yang et al. show similar behavior within an AgI-Cu catalyst, in which the I component is leached from the Ag nanoparticles, showing similarly impressive C_{2+} FE (Figure 9d).[197] The same iodine-leaching phenomenon was observed within the Ag nanoparticles, forming a diverse and active Ag interface for CO_2RR.

Other types of metal-nonmetal based catalysts have been investigated, like B-doped,[200] N-doped or N-coordinated,[61,196,201–203] CO_3-modified,[105] or Si-modified Cu species.[28] Ultimately, F-modified and I-modified Cu structures seem to have the most promise in high-performance operation, albeit for different reasons. While F-modified Cu seems to retain F within the structure of the catalyst throughout the reaction, I has consistently shown that once the reaction begins, the vast majority of the I present leaves the surface of the catalyst, instead improving the reactivity of the catalyst by introducing the formation of a rough surface texture.[54,105,199]

5.2. Surface Engineering Approaches

5.2.1. Electrochemical Alteration

Electrochemical treatment of catalysts during and before CO_2RR is conducted is an effective and facile strategy for electrocatalyst improvement, particularly for raising the ethylene FE by suppressing HER and developing a more focused CO_2RR reaction pathway.[71,204] Although electrochemical pretreatment has been a strategy utilized for many years across multiple fields, altering the electrochemical properties during the CO_2RR itself has emerged as a promising strategy for increasing the stability and the selectivity of these reaction systems.[113] By pulsing (i.e., regularly varying the potential) the electrodes during the reaction, some research has indicated that the catalyst surface "resets", in the sense that many of the adsorbed species desorb, allowing for the re-adsorption of reactant again.[113] Frequently, reactive sites can become deactivated by some unwanted species, not only blocking that site for reaction, but also lowering the surface concentration of the critical $*C_1$ intermediates.[180] Even beyond the adsorption of reactant species to the catalyst surface, the reorganization of the inner and outer Helmholtz layers can reduce the procession of electrowetting-induced flooding.[106] Additionally, during CO_2RR, the active catalyst surface defects may be removed, but by performing anodic pulses, they can be reformed.[101]

Meanwhile, pulsing reaction conditions have been shown by the Cuenya group to improve not only the ratio of C_{2+}/C_1 product formation but also the ratio of ethylene and ethanol formation by harnessing the induced nanostructure transformation (**Figure 10a**).[101,205] While the pulsing method initially seemed only to improve C_2H_5OH formation, further studies have also indicated possible benefits for ethylene formation. In their 2021 publication, Tang et al. used a generic (100)-textured Cu foil electrode to conduct CO_2RR with the hypothesis that the selectivity for a certain electrode type can be tuned by temperature and pulsed operation effects.[206] Indeed, not only did they find that using a pulsed electrode, CO_2RR conversion to C_{2+} products can be enhanced, but they also determined that lower temperatures facilitate greater ethanol formation on the surface of the catalyst during this pulsing process. Conversely, higher temperatures are more conducive to the creation of ethylene.[5,206,207] Additionally, electrochemical pulsing has been applied to prevent HER from occurring, as it has been shown to reduce the adsorption of *H species

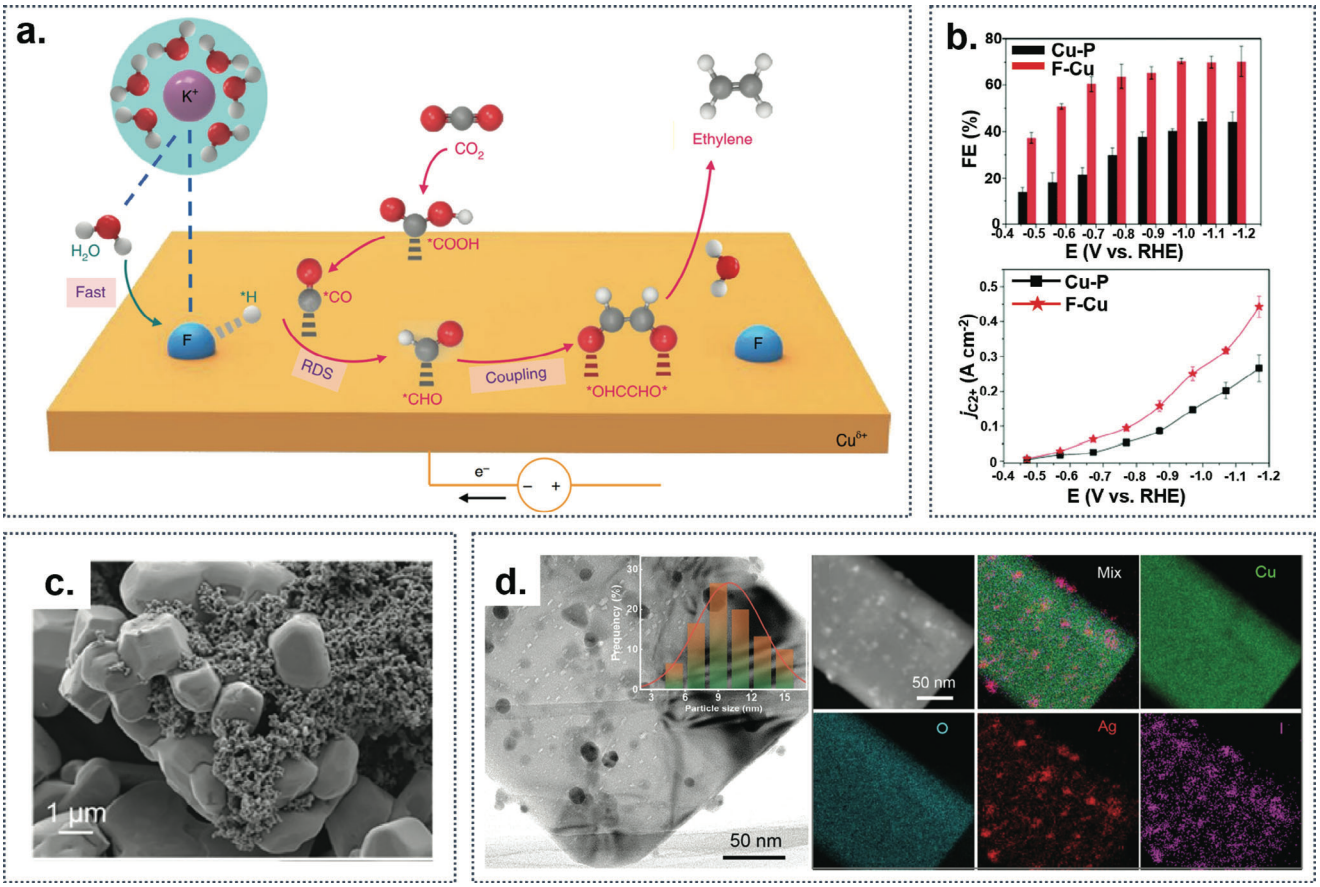

Figure 9. a) Conceptual depiction of the role of surface F on the production of ethylene via CO_2RR. Reproduced with permission.[54] Copyright 2020, Springer Nature. b) Comparison of the performance of a Cu-based catalyst both with and without F. Upper: FE_{C2+} measured as at various potentials within a GDE flow cell. Lower: C_{2+} partial current density measured at various potentials within a GDE flow cell. Reproduced with permission.[198] Copyright 2022, Royal Society of Chemistry. c) SEM image of Li et al.'s Cu/CuI catalyst. Reproduced with permission.[199] Copyright 2022, Wiley. d) HRTEM and EDX spectroscopy showing the AgI particle size and elemental distribution of Ruoou et al.'s Cu-AgI catalyst. Reproduced with permission.[197] Copyright 2021, Wiley.

on the surface of the catalyst relative to that of *CO.[206,208] To further corroborate the rest of the results reported in this section, Kim et al. showed that an optimized pulsed electrode system could simultaneously suppress HER, improve the ratio of C_2 to C_1 products, and also customize the ratio of ethylene to ethanol.[208]

Further, some researchers have explored pretreatment methods to enhance the cathode's properties for CO_2RR. Generally, these approaches relate to the exposure of the cathode to anodic conditions before the reaction to develop a more tuned or rough surface.[96] Lee et al. studied the effect of different anodization treatments on the characteristics of Cu-based CO_2RR catalysts, especially concerning the stability of the resulting material (Figure 10b).[209] Ultimately, they found that by carefully adjusting the process, the electronic state of the Cu species can be tuned, which results in a different product distribution within the CO_2RR. Studies have shown that by using a harsh electrochemical pretreatment process, higher stability and resistance to the reaction environment may be cultivated compared to mild treatments.[103,209] For instance, Lei et al. developed two Cu-based catalysts, one heat-quenched (HQ), and one anodized (AN), before exposing them to harsh electrochemical treatment (PHQ-Cu and PAN-Cu, respectively).[210] Mechanistically, they suggest that the elevated performance of the PAN-Cu and PHQ-Cu catalysts can be attributed to the formation of fragmented grain domains, which is reasonable based on the effect of grain boundaries on the C-C coupling step.[211] Importantly, the anodization current density should be meticulously selected to optimize the surface of the catalyst, which represents a method to produce effective catalysts in large quantities to improve the scalability of the process (Figure 10c).[27,103] Regardless, electrochemical pretreatment and tuning have been shown to increase the effectiveness for CO_2RR, particularly for enhancing the selectivity and the stability of the catalysts, and should be considered a fundamental approach for the design and optimization of new materials for CO_2RR applications. It should be noted that these surfaces all change drastically over the course of light anodization, so there are potentially more effective protocols that can be used to increase the quality of these reactive surfaces.

Certainly, electrodeposition is one of the most popular methods for producing Cu-based catalysts for CO_2RR due to its ability to form highly active catalysts with a very controllable and facile

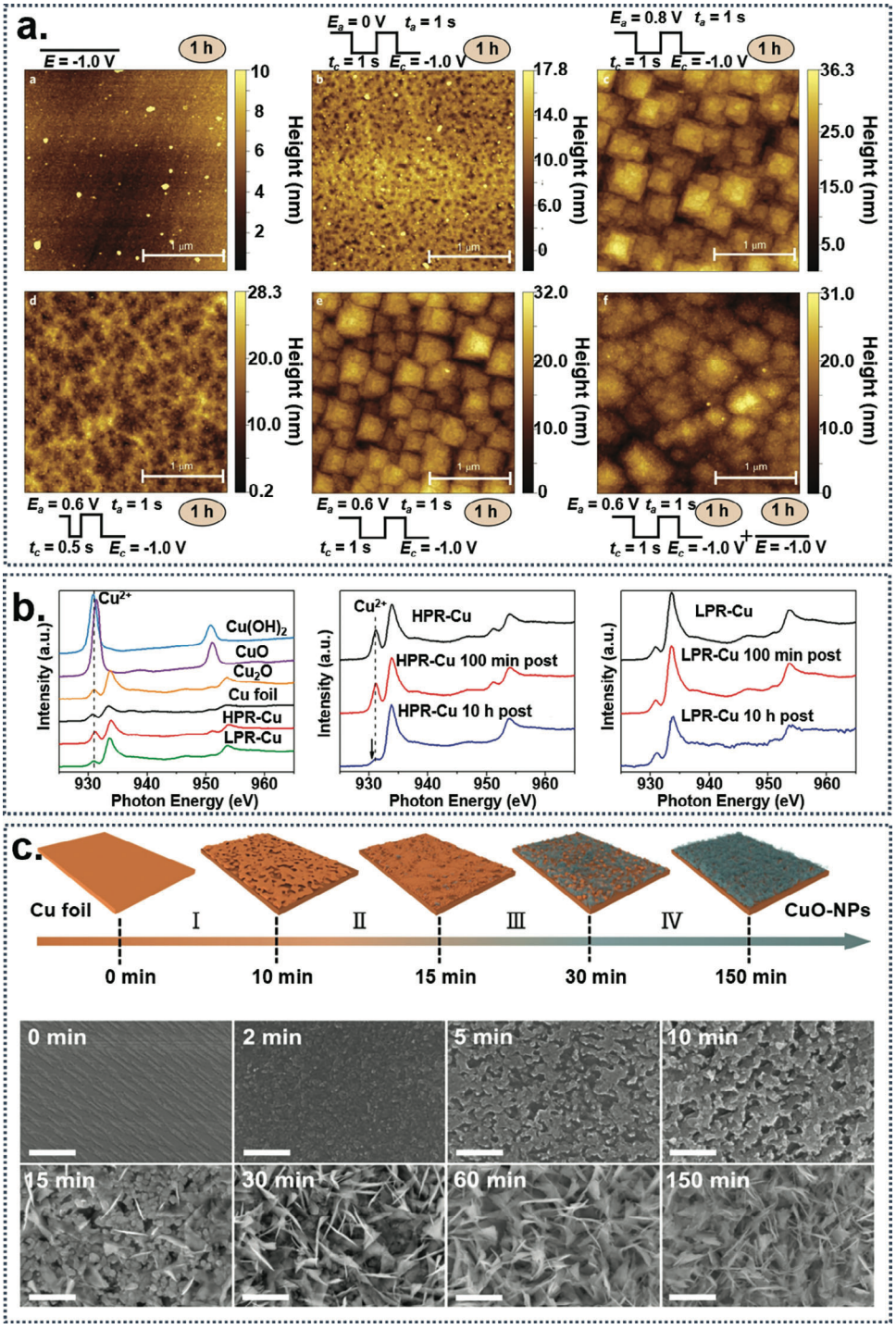

Figure 10. a) Atomic force microscopy images showing the surface morphology of a Cu (100) electrode after different pulse treatment protocols, detailed with each image. Reproduced with permission.[101] Copyright 2020, Springer Nature. b) Left: XANES spectra of Cu undergoing high (HPR) and low (LPR) potential reduction before CO_2RR. Middle: XANES spectra before CO_2RR, after 10 min of CO_2RR, and after 10 h of CO_2RR for HPR-Cu. Right: XANES spectra before CO_2RR, after 10 min of CO_2RR, and after 10 h of CO_2RR for LPR-Cu. Reproduced with permission.[209] Copyright 2018, American Chemical Society. c) Above: diagram depicting the electrochemical formation of CuO-NPs on the surface of Cu foil over time. Below: SEM images showing the surface morphology of Cu foil after an anodic oxidation process for a corresponding duration. Reproduced with permission.[96] Copyright 2022, Springer Nature.

method.[76] Adjusting the deposition system may make the process customized to encourage certain structures, with dendrites being a commonly formed geometry.[102,212,213] Fortunately, dendrites show high surface area and many interfaces for C-C coupling interaction and are conducive for this kind of application. Additionally, the process can be relatively easily transferred to large-scale syntheses by increasing the deposition area. However, the system is quite sensitive to changes in critical parameters, like current density, deposition electrolyte concentration, and voltage; for this reason, it may be challenging to ensure that the conditions are identical across the entire deposition surface.

5.2.2. Active Site Tuning

For reactions as complex as CO_2RR to C_{2+} products, ensuring the formation of ideal active sites is a chief concern for realizing efficient reduction of CO_2 with high selectivity for preferred products.[214,215] By altering the species at the catalyst's surface, certain reaction pathways may be promoted to allow for highly selective strategies using unique approaches. An increasingly promising method of doping the catalyst's surface with various species with the goal of perfecting the catalyst's adsorption and subsequent desorption behavior has begun to emerge. In essence, these molecules could direct and control the diffusion of unwanted species more rigorously than electrolyte ions in the Helmholtz layer alone, while concurrently providing optimal steric effects to adjust the intermediates formed by the reaction.[65,216,217] Furthermore, these structures can stabilize thermodynamically unfavorable intermediate adsorption orientations, allowing for tunable reaction pathways. For example, in a paper by Li et al., a Cu-SiO_x nanoparticle catalyst was synthesized using a modified conventional precipitation method to alter the surface of the catalyst such that the intermediates were sterically encouraged to progress down a specific reaction path.[28] Critically, the team used DFT calculations to determine that with the proper inclusion of SiO_x at the catalyst surface, the ethylene-selective carbon-coupled *OCCOH intermediate was encouraged, thus steering the reaction toward the preferential formation of ethylene.

The inclusion of different species at the catalyst surface has presented many impressive transformations of the product distribution for a catalyst. It has been shown that a dramatic increase in the ethylene selectivity of polycrystalline Cu could be achieved with the incorporation of imidazolium species on the surface of the catalyst, with an enhancement from 5% to 73% FE for ethylene following surface modification (**Figure 11**a,c).[218] This behavior can be ascribed to optimized CO_2 adsorption properties and imidazolium-assisted stabilization of certain intermediate species on the surface of the catalyst, which further facilitates CO_2-to-C_2H_4 electroconversion. Despite all the imidazolium-containing dopants studied possessing similar structures and identical moieties, dramatic differences were observed in the performance of the catalysts obtained.[218] This effect can be found in many N-containing surface dopants, such as amines and other components,[64,219–222] and can ultimately be understood as intermediate and reactant stabilization assistance.[223] Finally, Chen et al. developed a Cu-polymer catalyst with an impressive 87% FE for ethylene and 93% FE for C_{2+} products overall by including polyamine species on the catalyst's surface (Figure 11b).[41] The authors posit that the addition of polyamine to the catalyst increases the surface pH, thereby enhancing the *CO content as well as the intermediate stability due to the entrapment of these species at the surface while also reducing the favorability of HER, ultimately reducing the cathodic overpotential to just −0.47 V versus RHE, with an ethylene onset potential of −0.17 V versus RHE. The utilization of molecules within the catalyst structure is perhaps one of the most promising directions for high-efficiency C_{2+} formation, as the customizability of the incorporated species is incredibly high and allows for careful tweaking of adsorption properties.[224,225] Alternatively, large-scale diffusion layers like the catalyst-ionomer planar heterojunction (CIPH) concept developed by García de Arquer et al. have shown promise by utilizing a similar strategy (Figure 11d).[16] The developed catalyst relies on a coated ionomer layer atop the Cu catalyst surface, facilitating extremely efficient mass transfer behavior by dramatically enhancing gaseous mass transfer concerning liquid transport.[226] Ultimately, the benefits of this strategy are twofold: not only is the current density of the catalyst increased, but HER is suppressed as well.

Inducing the creation of surface defects on the surface of electrocatalysts for CO_2RR has also enhanced ethylene conversion performance.[227] Sun et al. showed a catalyst with high C_{2+} efficiency due to the high density of grain boundary defects at the catalyst surface (**Figure 12**a).[228] In 2019, Mi et al. reported a Cu_3N electrode with many surface defects, such as grain boundaries and vacancies, leading to improved ethylene formation.[196] The following year, Zhang et al. produced a nanodefect-rich Cu nanosheet catalyst, which showed an 83% ethylene FE, which was better than their samples with reduced nanodefective character (Figure 12b).[42,229,230] The inclusion of surface defects is one of the more common methods for increasing the performance of these catalysts, with numerous examples of the inclusion of grain boundary-rich Cu surfaces or irregular electrochemically modified Cu surfaces.[69,210,228,231] These surface defects enhance the catalyst's reactivity by increasing the surface energy and altering the adsorption properties, which serves to localize and arrange $*C_1$ intermediates such that C-C coupling is enhanced. Alternatively, significantly different surface morphologies were obtained simply by adjusting the Cu salt type inside an electrochemical synthesis (Figure 12c).[105] Thus, there are numerous ways to tune and tweak the surface morphology of Cu-based catalysts, which have been shown to impact the CO_2RR activity positively.[232]

Porosity predictably plays an influential role in all catalytic systems. However, there is an added layer of influence in complex and extended mechanisms like CO_2-to-C_{2+} conversion. Small pores may enhance the formation of C_{2+} catalysts by confining the reaction intermediates to the surface of the catalyst, reducing the rate at which unfinished $*C_1$ species are desorbed from the catalyst surface despite middling reactant binding strength of the active sites.[42,105] Morphological engineering studies have shown incredible control over pore structure for catalysts within the CO_2RR. Particularly, it was shown by Zhang et al. how the size of nanocavities within an engineered CuO catalyst can encourage the formation of either ethylene or ethanol (Figure 12d).[91] The nanocavity structures were presumed to have a confinement effect that promotes one pathway over the other. This approach

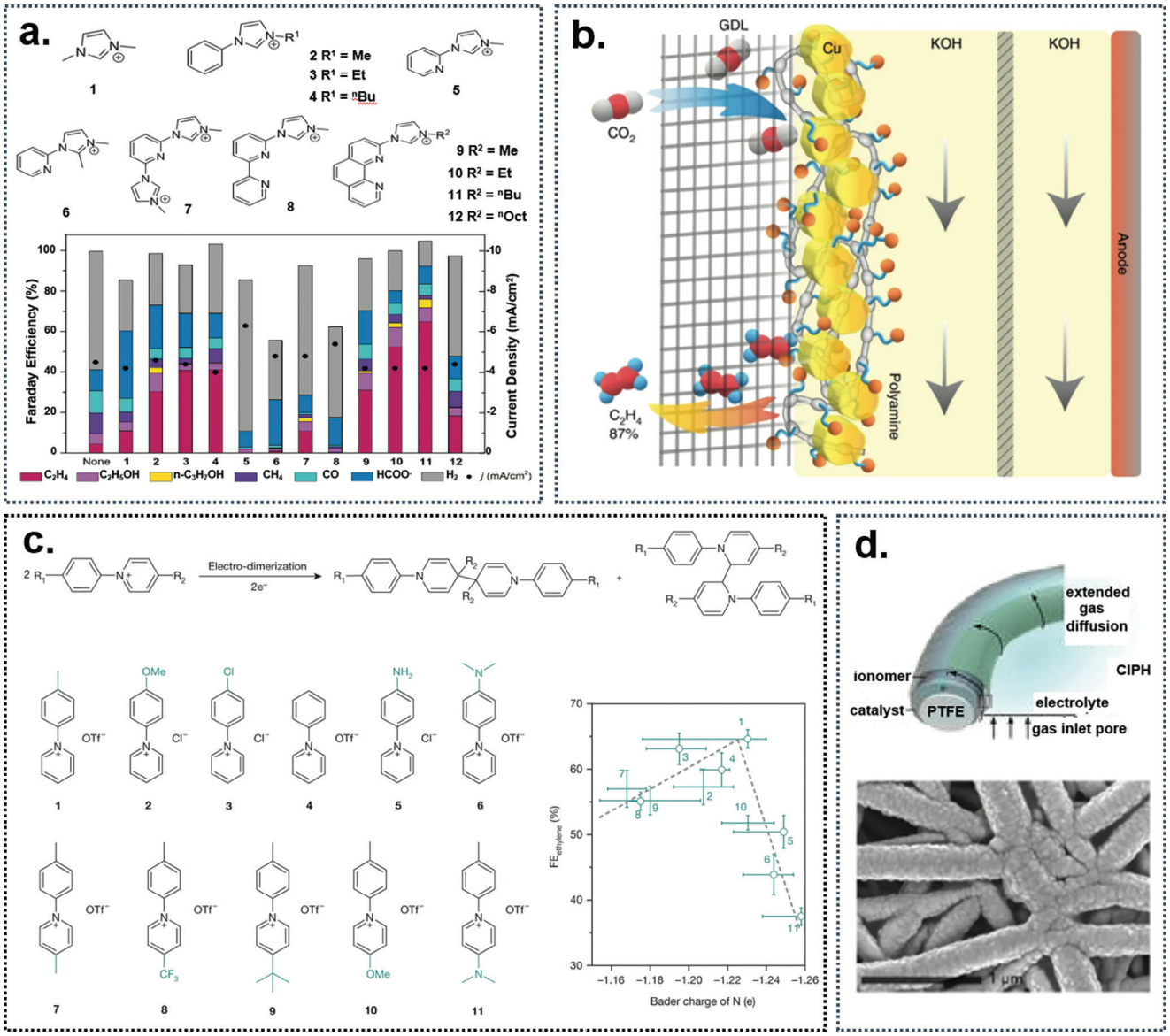

Figure 11. a) FEs and current densities of 12 varieties of imidazolium-modified polycrystalline Cu electrodes.[218] b) Diagram depicting Chen et al.'s polyamine-incorporated Cu electrode in a flow cell system. Reproduced with permission.[41] Copyright 2020, Springer Nature. c) Various pyridinic N additives utilized, along with the effect of the N Bader charge on the ethylene FE. Reproduced with permission.[65] Copyright 2019, Springer Nature. d) Upper: conceptual depiction of the CIPH strategy developed by the Sargent group to regulate the local pH environment inside of MEA configurations. Lower: SEM images of the CIPH Cu catalyst. Reproduced with permission.[16] Copyright 2020, The American Association for the Advancement of Science.

resulted in defective sites within the pores that further elevate the catalyst's performance by forming the morphologically driven adsorption strength gradients discussed previously.[42,231] Other nanostructured catalysts, like Cu nanowires, meshes, and single-atom Cu catalysts, have been investigated.[195,202,233,234]

Due to Cu's favorable adsorption properties, nanostructured and nanodefective Cu is perhaps the most thoroughly studied catalyst morphology for forming C_{2+} species via CO_2RR.[74,235] In essence, nanodefective and nanostructured catalysts function similarly since $*C_1$ intermediates will localize around boundary areas between regions of different adsorption energies, which can be achieved by either defect introduction or samples that contain multiple crystallographic Cu facets.[42] For single-crystal surfaces, it has been found that Cu (100) is more effective than Cu (110) and Cu (111) for producing ethylene, albeit with low FE.[236–238] In contrast, catalysts with multiple crystal faces have been shown to provide a method of breaking the linear scaling relationship of adsorption strength within CO_2RR. For instance, a classic example of effective CO_2-to-C_2H_4 catalysis is the usage of Cu_2O nanocubes, which possess a different crystallographic phase on the faces (100) instead of the edges (110).[72] Modeling studies have suggested a synergistic effect exists between these two regions, with the faces having the ability to make *CO efficiently, while the edges can promote the C-C coupling step.[27] From a mechanistic perspective, the transport of C_1 intermediates from the faces to the edges of the nanocubes is critical for

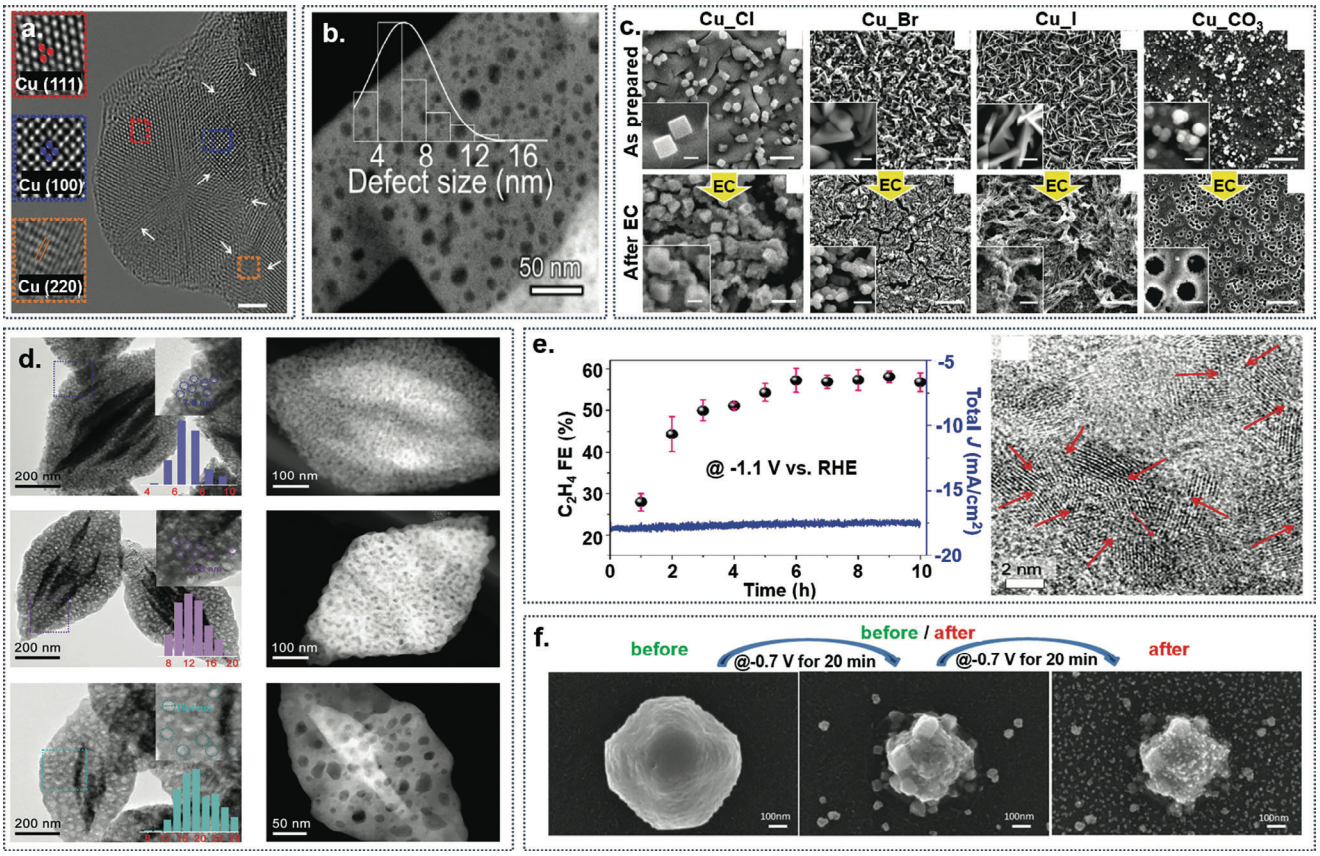

Figure 12. a) TEM image of Sun et al.'s KB@Cu_3(HITP)$_2$ electrode after undergoing 10 h of CO_2RR at −1.25 V versus RHE. Reproduced with permission.[228] Copyright 2021, Springer Nature. b) HAADF-STEM image of Zhang et al.'s n-CuNS catalyst, with inset detailing the size distribution of the defects. Reproduced with permission.[42] Copyright 2020, American Chemical Society. c) SEM images of four different Cu-based catalysts formed by electrodeposition in different Cu-based solutions (from left to right: CuCl, CuBr, CuI, and $CuCO_3$). Upper: SM images before CO_2RR. Lower: SEM images after CO_2RR. Reproduced with permission.[105] Copyright 2019, Wiley. d) HRTEM images of a CuO catalyst containing well-controlled, differently sized nanocavities. Reproduced with permission.[91] Copyright 2022, National Academy of Sciences. e) Left: FE and the current density of Jung et al.'s Cu-based NP/C catalyst show an increase in $FE_{ethylene}$ during the reaction. Right: HRTEM image depicting the Cu-based NP/C catalyst after 10 h of CO_2RR. Reproduced with permission.[211] Copyright 2019, American Chemical Society. f) Ex-situ SEM images of the proposed dissolution/redeposition process of degradation for Cu NPs after electrochemical treatment at −0.7 V versus RHE for 20 min and 30 min, respectively. Reproduced with permission.[98] Copyright 2021, Wiley.

the overall success of the catalyst, since the change in adsorption energy at the edges of the cubic structure serves to lower the activation energy of the C-C coupling step.[72] Researchers have developed a stronger understanding of the precise characteristics of Cu_2O nanocubes that promote reactivity and selectivity, like their size and composition.[72,115,201,239] Ultimately, raw Cu_2O nanocubes are outperformed by other catalysts that use them as a template to enhance the performance they provide, either by creating further customized nanostructures or by altering the environment in which they are tested,[102,228,240] which will be discussed in the next section. While it is true that these multi-faceted structures generally outperform single-crystal catalysts, there has also been data to suggest that high-index Cu facets can efficiently form C_{2+} species.[70,73] High-index facets expose a diverse set of Cu atoms that possess different energies and adsorption properties, which could explain their elevated performance in relation to more simple lattices.

Critically, the surface Cu nanostructures are often changed during CO_2RR, with some degree of reconstruction being expected. Usually, this reconstruction will expose new facets as active sites, which must be taken into account when determining why a catalyst may or may not be performing well.[217,241] This fact is essential for researchers to consider, boosting the usefulness of in situ observation techniques to help better describe the actual conditions of the reaction. This effect can sometimes be beneficial, as evidenced by the aforementioned electrochemical pretreatment method for enhancing performance. For example, catalysts that take advantage of the surface fragmentation effect often see an improvement in C_{2+} formation due to an increase in the density of grain boundaries.[242–244] The Kanan group illustrated this effect, showing that an increase in grain boundaries improved the rate of CORR while not influencing HER.[243] Further, they discovered a relationship between the microstrain strength and the grain boundary density, which could suggest that the fundamental cause of the enhancement is instead owed to the internal surface forces. Similarly, Jung et al. further demonstrated this effect by electrochemically fragmenting nanoparticles to increase grain boundary density; their catalyst exhibited

a gradual increase in C_2H_4 FE before stabilizing at ≈57% (Figure 12e).[211] Additionally, instances where ions are removed from the surface during the reaction have shown improved performance, such as halogen-leached Cu catalysts.[105,197,199] For example, Yang et al. showed a halogen-leached Cu oxide-based catalyst that produced a much more diverse set of exposed crystal facets after the reaction.[197] Obtaining a more comprehensive and deep understanding of the mechanisms driving these processes may allow for facile syntheses that result in very high performance.

Still, reconstruction can often deactivate the catalyst by harming the integrity of the support or by negatively impacting the valence state of the Cu active species, resulting in poor stability within the first few hours of operation. The common causes for this reconstruction are potential application, electrolyte effects, and oxidation of the Cu surface.[98] Potential-driven reconstruction is unavoidable for CO_2RR catalysts, and has been shown to have a profound effect on the structure of certain catalyst morphologies.[227] This process generally progresses as the dissolution and redeposition of Cu, as seen in Figure 12f.[98,100] Researchers often aim to create highly stable catalysts that do not show obvious signs of surface reconstruction after reaction, but these reconstruction mechanisms may be taken advantage of and allow for stable and highly active Cu catalysts. Alternatively, for multimetallic alloys, spontaneous phase separation likely occurs during CO_2RR operation, changing the structure of the catalyst surface, representing a fundamental challenge for applying multimetallic strategies toward CO_2RR.[245]

5.3. Reaction Environment Optimization

5.3.1. Operating Temperature

In general, room temperature operation seems to be an ideal selection for the formation of ethylene, with low temperatures being optimal for highly reduced C_1 products and high temperatures facilitating HER.[135,246] As previously discussed, Tang et al. studied the ambient temperature's effect on the performance of their pulsed electrode, which displayed a positive correlation between the ratio of hydrocarbons to oxygenates and the temperature.[206] Their optimal ethylene temperature was determined to be 25 °C, which is only slightly higher than a typical room temperature. Further, Ahn et al. conducted a similar experiment in examining how the temperature affects the selectivity of their catalyst but across a wider temperature range, observing high *CO coverage but low coupling ability at 2 °C, high *CO coverage, and decent coupling ability at 22 °C, and low *CO coverage and high HER at 42 °C (**Figure 13a**).[207] For this reason, temperature effects on CO_2RR have not been a research subject in recent years despite having a profound impact on selectivity, simply because the ideal temperature conveniently is near room temperature.

5.3.2. Operating Pressure

Absolute CO_2 feed pressure can impact the efficiency of electrolyzers by increasing the availability of the reactant gas. In the case of CO_2RR, this effect has been recorded extensively for CO-selective systems, which suggests that higher pressures are more conducive for higher FE_{CO}.[250–252] The rationale behind this behavior may be explained by an increase in CO_2 diffusion to the catalyst surface, thereby increasing the amount of active sites occupied by CO_2 and reducing the active sites occupied by H.[250] In principle, this phenomenon is rather intuitive, but other research has shown that increasing pressure has decreased the selectivity for CO, instead promoting the formation of HCOOH.[253] In the case of C_{2+} products, little research has been conducted regarding the effect of absolute pressure. However, some recent research has indicated that iso-propanol and ethanol formation rate can be improved using high pressures, showing reduced ethylene formation rate at higher pressures.[254,255]

CO_2 partial pressure shows interesting behavior when examining its effect on selectivity. Based on the work of Song et al., the optimal CO_2 partial pressure is correlated with the overpotential and current density.[256] The underlying mechanism behind this behavior is related to the $*CO_2$ coverage at the surface of the catalyst, since if the CO_2 coverage is too high, the C-C coupling step may be inhibited due to an absence of suitable coupling partners. Thus, it was found that at lower overpotential, a lower partial pressure of CO_2 maximized the $FE_{ethylene}$, whereas higher partial pressures resulted in the formation of excess CO.[256] Beyond the usage of pure CO_2/inert streams, CO_2/CO co-streams have been investigated as well, which predictably allow for the enhancement of C_{2+} product synthesis.[68,257] Contrarily, other studies have shown that increasing the ratio of CO to CO_2 in these co-feeds results in a selectivity profile shift, such as from ethylene to acetate.[258] More research should be done to determine how these aspects can affect the overall performance of CO_2RR electrolyzers.

5.3.3. Electrolyte Selection

The selection of a proper electrolyte and molarity has been under debate and development for some time. Recently, impressive results from increasing the molarity of commonly used KOH electrolytes have shown that high alkalinity electrolytes can promote the electrochemical performance of CO_2RR. In the aforementioned report from Chen et al., the effect of changing the molarity of the KOH electrolyte was observed and profound enhancements in ethylene FE (72% to 87%), overpotential (−0.97 V to −0.47 V), and onset potential (−0.47 V to −0.17 V) were recorded thanks to a higher surface pH, which further facilitated the stabilization of intermediates and the improved the *CO coverage of their polyamine-incorporated Cu catalyst.[41] Further, it has been shown that the local pH at the surface of a C;O_2RR catalyst is higher than that of the bulk electrolyte due to the consumption of protons and the attraction of OH^- ions.[259,260]

These results are corroborated by García de Arquer et al. and Dinh et al., both of whom achieved an increase in catalyst performance as a result of raising the molarity of the electrolyte being used. In particular, Dinh et al. reported a sputtered Cu-based PTFE catalyst that achieved 70% ethylene FE at current densities ranging from 275 to 750 mA cm^{-2}, with remarkably low onset potentials of −0.11 V for CO and −0.165 V for ethylene and stable operation for 150 h (Figure 13b).[97] As discussed, there must

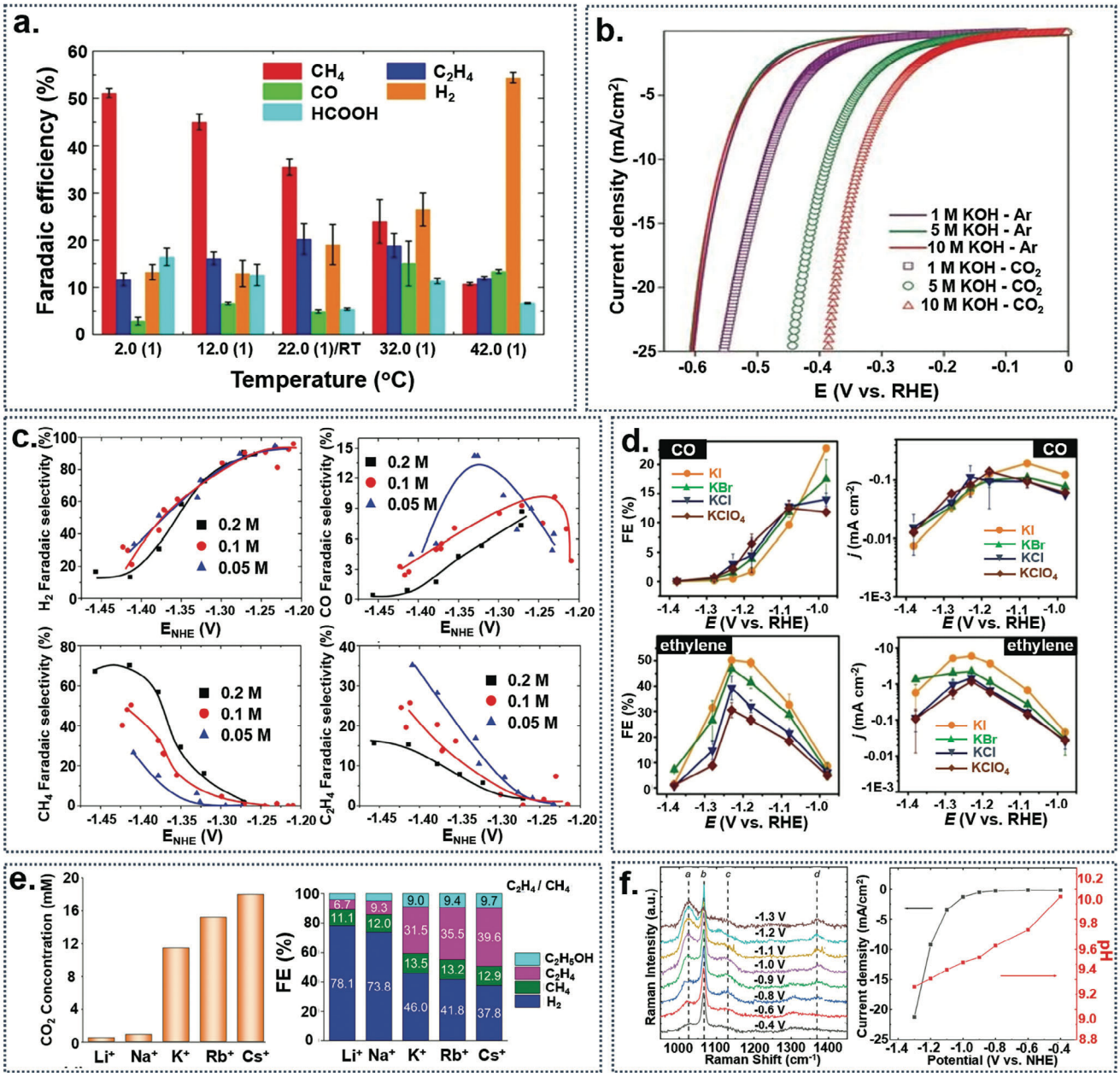

Figure 13. a) Effect of the reaction temperature on the FE of CO_2RR. Reproduced with permission.[207] Copyright 2017, Elsevier. b) Linear sweep voltammetry tests depicting the effect of the molarity of a KOH electrolyte on the current density of low-overpotential CO_2 reduction. Reproduced with permission.[97] Copyright 2018, The American Association for the Advancement of Science. c) Various FEs obtained via CO_2RR for a Cu catalyst in varied concentrations of $KHCO_3$ electrolyte. Reproduced with permission.[247] Copyright 2016, Elsevier. d) FE effect of different types of electrolytic anions contained within K-based electrolytes. Reproduced with permission.[248] Copyright 2018, Wiley. e) Left: product distribution of a Cu catalyst in different cations within -OH based electrolytes. Right: effect of the cation within -OH based electrolytes on the concentration of CO_2 at the surface of a Cu cathode. Reproduced with permission.[249] Copyright 2019, American Chemical Society. f) Left: surface-enhanced Raman spectroscopy (SERS) data showing a Cu-based catalyst's response to shifting applied potentials. Peak a represents $KHCO_3$, peak b represents K_2CO_3. Right: current density and electrolyte pH for a Cu catalyst when exposed to different potentials. Reproduced with permisssion.[94] Copyright 2021, American Chemical Society.

necessarily be some gap between the onset potentials for each, but the dramatic increase in the pH of the electrolyte significantly shrunk the difference due to the very inefficient *CO desorption rate from OH^- ion blockages at the surface of the catalyst. Further, these OH^- ions interact with the intermediates and promote C-C coupling due to induced dipoles on C atoms from the highly negatively charged electrolyte in relation to the positively charged cathode. Importantly, potentials in this range are low even for HER, meaning that the voltage applied to the catalyst in these systems may not be enough to facilitate HER side reaction. In terms of electrolyte selection, they found that KOH was indeed the most optimal electrolyte for their system. Parallel to these

results, decreasing the concentration of more acidic electrolytes has also been found to increase the selectivity for ethylene, indicating that neutral electrolytes will likely need to be relatively dilute to obtain high-performance C_{2+} formation (Figure 13c).[247] Although high pH electrolytes have been shown to allow for better product selectivity, there are still major reasons for increasing the efficiency of neutral and acidic electrolytes. Specifically, using an alkaline electrolyzer for CO_2RR has fundamental challenges regarding system stability due to the precipitation of salts within the GDL and inside the gas flow field, not to mention CO_2 crossover. Furthermore, within high-efficiency zero-gap MEA configurations, the IEM interfaces directly with the catalyst surface. PEMs generally outperform AEMs due to a smaller ion size and more efficient ion permeability. However, this is currently a major issue due to catalysts having an intolerance for low pH environments.

However, the selection of certain electrolytes has been shown to affect the procession of HER on CO_2RR electrocatalysts. Namely, KCl and K_2SO_4 have been shown to adsorb more strongly to the catalyst surface and prevent the adsorption of H to the surface, thereby increasing the surface pH of the catalyst.[54,96] A chief concern for the electrolyte is the formation of an ideal inner/outer Helmholtz layer and electrolytes like KCl or $KHCO_3$ can be used to adjust the properties of the adsorption of species to the surface of the catalyst.[261] In a study by Huang et al., the effect of the type of electrolyte anion (Cl^-, Br^-, I^-, and ClO_4^-) was analyzed, showing enhanced FEs for ethylene when KI and KBr were utilized (Figure 13d).[248] Based on in situ Raman spectroscopy, the authors concluded that a red shift of varying strength existed in the C-O stretching band depending on the electrolyte used, indicating a weakened vibrational energy. This red shift correlated with the production of C_{2+} species across the different electrolytes on the order of KI > KBr > KCl > $KClO_4$, suggesting that the local binding environment was adjusted based on the anionic species used. Alternatively, different cation components may be utilized for CO_2RR, which show a distinct ability to suppress HER. It has been found that Li- and Na-based bicarbonate electrolytes are poor for the enhancement of CO_2RR due to rampant gaseous H_2 formation, whereas larger group 1 metals like K, Rb, and Cs all improve CO_2RR (Figure 13e).[249] The reasoning for this behavior can be understood by examining the effect of the cations within the outer Helmholtz layer, which shows a relationship between the cation size, local pH, and the concentration of CO_2 at the surface of the catalyst.[249] Specifically, small ions like Li^+ and Na^+ coordinate with the water molecules within the Helmholtz layer and reduce the buffering capability of the electrolyte at the catalyst surface. Meanwhile, larger ions like K^+, Cs^+, and Rb^+ all possess a higher pK_a for hydrolysis, allowing the electrolyte at the surface to have a higher CO_2 concentration, thereby enhancing CO_2RR and suppressing HER. Similarly, it has been found that potential application on Cu electrodes also induces a negative pH shift as the potential magnitude increases, all of which may have a direct impact on the catalyst structure (Figure 13f).[94] The change in pH is unrelated to the progression of CO_2RR, since the pH reduces before the onset of CO_2RR. Thus, this behavior is likely due to the alteration of the Cu surface itself, which the authors attribute to the formation of a thin malachite ($Cu_2CO_3[OH]_2$) phase on the surface of the electrode. The presence of a CO_3^{2-} layer atop the electrode decreases the local pH even when there is no CO_2RR taking place within KOH electrolyte. Obtained surface-enhanced Raman spectroscopy w(SERS) spectra support this claim, showing the depletion of $KHCO_3$ and replacement with K_2CO_3 peaks as the applied potential becomes more negative. There remains opportunity to investigate the role of the electrolyte within CO_2RR, such as using new electrolytes as well as mixed electrolytes to increase the efficiency.[157,234,262]

CO_2RR taking place in acidic conditions is a major challenge, however there are promising results that indicate it still is possible to obtain high-efficiency conversion. A fundamental problem with using neutral and basic electrolytes in for the CO_2RR is the loss of CO_2 to CO_3^{2-} formation, which becomes highly problematic for extended reaction mechanisms like C_2H_4 formation.[215] Concurrently, neutral and alkaline electrolytes allow for the transfer of species across the AEM, resulting in the loss of liquid product.[133] Although this is not particularly relevant for C_2H_4 in isolation, any C_{2+} product formation usually results in the formation of multiple types; thus, part of the value of a CO_2-to-C_2H_4 electrolyzer lies in the formation of these liquid products (ethanol, acetate, etc.).[14,150] The crossover of liquid products and generation of excess CO_3^{2-} in the electrolyte hampers the SPC of the system overall.[154] Further, if these lost products and CO_2 stored as CO_3^{2-} are to be recovered from the electrolyte, additional processing is required that increases the costs associated with C_2H_4 production.[154] The challenge lies in the suppression of HER, but has been shown to be achievable through the rational design of catalyst materials, even in systems looking to produce C_2H_4.[168,263,264]

6. Summary and Current Perspective

CO_2RR remains a challenging but enticing technology for controlling the effects of utilizing anthropogenic energy sources on the atmosphere. Currently, CO electrosynthesis remains the most applicable variety of CO_2RR thanks to its relatively low complexity and natural HER suppression due to its equilibrium potential.[8,14,265] Nevertheless, dramatic progress has been made toward allowing for efficient ethylene formation through CO_2RR, which is much more environmentally friendly when compared to steam cracking, the current industrial method for ethylene synthesis. With the advancement of CO_2-to-ethylene conversion, it is possible to simultaneously reduce CO_2 emissions and eliminate a current source of CO_2 emission by replacing it with CO_2RR. Naturally, this will take time and concerted effort from researchers to develop new strategies in designing efficient ethylene electrosynthesis systems.

There are many avenues that can be taken to improve the performance of ethylene selective CO_2RR electrocatalysts, however, these changes typically relate to only a few properties. As discussed previously, the key challenge for CO_2RR toward C_{2+} is selectivity, both in obtaining a specific CO_2RR product and suppressing the formation of H_2 via HER. Plenty of different methods have been developed for modulating the selectivity of catalyst surfaces, but in principle, these approaches generally affect the same characteristic: adsorption strength. Adsorption strength represents the most critical component for C_{2+} product formation, as creating a high surface concentration of available and mobile $*C_1$ intermediates is critical for producing

C_{2+} species.[21,27,55] While Cu is the only material that has been observed to possess the electronic structure necessary for this application, there are a plethora of novel strategies recently developed by researchers to organize an ideal surface state with abundant $*C_1$ intermediates. Due to the narrow potential range for C_{2+} products, overpotential does not have a strong impact on the distribution of multicarbon products, meaning that the catalyst must be rationally designed in such a way that the undesirable reaction pathways are effectively discouraged. Although C_{2+} formation does necessarily require higher overpotential when compared to lightly reduced C_1 species, in many cases, the limiting parameter is actually the concentration of $*C_1$ on the surface rather than the energetic requirements. Thus, by maintaining a high concentration of $*C_1$, the overpotential necessary to form C_{2+} species can be reduced and, by extension, the energy requirement.

The reduction of overpotential has many interesting consequences on practical CO_2RR applications beyond simply allowing for lower energy usage. For the high-current, industrially applicable cell configurations, a GDL is necessary for allowing ideal interaction between the solid catalyst surface, liquid electrolyte phase, and gaseous CO_2 reactant. Due to potential application during CO_2RR, the hydrophobic GDL may become hydrophilic through an electrowetting process, interrupting the formation of the desired triple-phase interface.[107] The severity of this electrowetting phenomenon is directly correlated with the magnitude of the potential applied, suggesting that by lowering the necessary potential application, the system stability of the reactor as a whole may be enhanced. Additionally, by reducing the required potential for the formation of the desired CO_2RR product, typically the progression of HER will be suppressed simply due to the expansion of their equilibrium potential difference.

Unfortunately, another key challenge for applying CO_2RR within industrial settings is its application in flow-type cell configurations and MEAs. While the integrity of the GDL may be preserved by lowering the applied potential, CO_2RR catalysts thus far have primarily been designed and optimized within alkaline conditions. Given the competitive HER side reaction, alkaline conditions naturally allow for a higher preference for the desired CO_2RR product.[97] Within MEAs, the CO_2RR catalysts are typically deposited and interface with the IEM directly; however, current AEMs are not as efficient as PEMs due to the transfer of heavier hydroxide ions rather than very small protons, not to mention significant issues with CO_2 utilization and SPC.[106,112] While operating an MEA electrolyzer with an AEM is possible, the overall resistance within the cell is elevated, and more importantly, CO_2 crossover becomes a significant concern.[266,267] Ideally, CO_2RR catalysts would be improved to a point where HER progression becomes highly suppressed, allowing for operation in low pH conditions. Some progress has been made with applying lightly reduced C_1 products within acidic electrolytes. However, conducting C_{2+} electrosynthesis in acidic environments has been challenging.[167]

Additionally, stable performance has been mostly neglected as a primary concern for CO_2RR catalysts. Regarding industrial application, high stability catalysts are imperative for the eventual

Table 2. Summarization of a selection of high-performance ethylene selective CO_2RR catalysts. The potential reported for MEA-style electrochemical cells is in terms of overall cell voltage, whereas in cathodic potential for H- and flow- configurations.

Catalyst Name	FE [%]			Current Density [mA cm^{-2}]	Potential [V vs RHE]	Lifetime [h]	Cell Type	Refs.
	C_2H_4	C_{2+}	H_2					
CuO/Al_2CuO_4	70.1	71	11	600	-2.031	100	GDE	[15]
PTFE with Cu and CNPs	66	83	5	275	-0.54	150	GDE	[97]
DVL Cu	84.5	85	10	200	-0.8	55	GDE	[96]
Polyamine entrained Cu	72	90	3	433	-0.97	3	GDE	[41]
Cu(OH)F	65	80	6	1600	-0.89	40	GDE	[54]
Cu/CuI	33	71	11	894	-1.0	85	GDE	[199]
3D Cu mesh	58	65	15	527	-1.2	10	GDE	[234]
Cu-TABQ	53.1	63.2	20	423	-1.17	10	GDE	[202]
Electrodeposited CuAg	60	85	10	300	-0.7	–	GDE	[76]
Organosuperbase Cu	50	80	10	200	-1.1	7.5	GDE	[225]
$Cu(OH)_2$-D	58	87	8	250	-0.54	10	GDE	[71]
CuI	45	80	22	39	-0.9	–	H	[105]
Branched Cu NPs	70	70	30	30	-1.05	12	H	[102]
Nanodefected Cu	83	83	16	65	-1.18	14	H	[42]
Pulsed Cu cathode	42	81	11	14	-0.8	–	H	[208]
Self-cleaning Cu NPs	55	80	–	138	-3.8	157	MEA	[113]
Cu-KOH	54.5	78.7	–	281	-3.25	6	MEA	[136]
Cu-CTPI	66	–	–	315	-3.9	100	MEA	[110]
Standard Cu with CIPH	52	–	10	1000	-3.9	60	MEA	[16]
Cu-SiO_x-2.5	64	–	13	300	-4.2	55	MEA	[28]
Cu-12	64	–	8	600	-3.65	190	MEA	[65]

application of CO_2RR at large-scale. Overall, more effort should be dedicated to identifying the degradation mechanisms relevant to CO_2RR. From a catalyst surface perspective, Cu-based materials have a weakness in that they are easily oxidized and tend to reconstruct relatively easily.[5,98] Therefore, new strategies to assist in maintaining Cu electrode structure are a valuable and promising path toward realizing high-stability Cu-based CO_2RR systems. Crucially, the stability of these CO_2RR systems depends not only on robust catalyst structure but also on the stability of the components within the reactor system. Researchers should also consider optimizing the efficiency of the reactor components' to prevent processes like flooding or the deposition of bicarbonate salts within GDLs. Furthermore, additional work should be dedicated to developing techniques to allow the marriage of CO_2RR and MEA function to prevent challenges like CO_2 crossover during operation, which can harm stability, CO_2 utilization, and overall performance.[266,268]

A variety of effective methods have been demonstrated to positively impact the catalyst and system properties of CO_2-to-ethylene processes, and a selection of the most notable examples has been organized and tabulated in **Table 2**. Throughout this review, we have discussed the principles and concerns related to CO_2RR, the benchmarks required of CO_2RR technology, the governing conditions that guide CO_2 electroreduction, and the effective strategies implemented by scientists to utilize these fundamental principles of CO_2RR to fabricate efficient and effective electrocatalysts. These strategies may be built upon further to produce more optimized catalyst variations and combined to manufacture an ideal reaction system for promoting ethylene. CO_2RR as a field of study is in a critical stage of development, where the mechanisms and extent to which conditions affect these mechanisms are not fully understood due to the elaborate and convoluted CO_2RR pathways. However, powerful in situ observation protocols and accessible advanced DFT analysis techniques have recently allowed for a much deeper understanding of the influence of $*C_1$ intermediate formation.[55,261,269] Nevertheless, more progress is needed for implementing ethylene-selective CO_2RR in industrial settings, which represents a large step toward remedying the current climate crisis faced by the world today. This improvement should be considered holistically, such that both CO_2RR reactor conditions and catalyst design work in tandem to enable high-efficiency ethylene electrosynthesis.

Acknowledgements

The authors thank the support from the New York State's Center of Excellence in Materials Informatics (CMI) at the University at Buffalo and the National Science Foundation (CBET-1804326). L.F. acknowledges the National Science Foundation (2119688).

Conflict of Interest

The authors declare no conflict of interest.

Keywords

CO_2 electroreduction, Cu electrocatalysts, electrocatalysis, ethylene electrosynthesis

Received: April 7, 2024
Revised: May 23, 2024
Published online: June 11, 2024

[1] E. A. G. Schuur, A. D. McGuire, C. Schädel, G. Grosse, J. W. Harden, D. J. Hayes, G. Hugelius, C. D. Koven, P. Kuhry, D. M. Lawrence, S. M. Natali, D. Olefeldt, V. E. Romanovsky, K. Schaefer, M. R. Turetsky, C. C. Treat, J. E. Vonk, *Nature* **2015**, *520*, 171.
[2] S. Solomon, G.-K. Plattner, R. Knutti, P. Friedlingstein, *Proc. Natl. Acad. Sci. USA* **2009**, *106*, 1704.
[3] R. Lin, J. Guo, X. Li, P. Patel, A. Seifitokaldani, *Catalysts* **2020**, *10*, 473.
[4] Z.-Z. Niu, L.-P. Chi, R. Liu, Z. Chen, M.-R. Gao, *Energy Environ. Sci.* **2021**, *14*, 4169.
[5] S. Nitopi, E. Bertheussen, S. B. Scott, X. Liu, A. K. Engstfeld, S. Horch, B. Seger, I. E. L. Stephens, K. Chan, C. Hahn, J. K. Nørskov, T. F. Jaramillo, I. Chorkendorff, *Chem. Rev.* **2019**, *119*, 7610.
[6] H. Tabassum, X. Yang, R. Zou, G. Wu, *Chem Catalysis* **2022**, *2*, 1561.
[7] F. Pan, X. Yang, T. O'Carroll, H. Li, K.-J. Chen, G. Wu, *Adv. Energy Mater.* **2022**, *12*, 2200586.
[8] O. S. Bushuyev, P. De Luna, C. T. Dinh, L. Tao, G. Saur, J. van de Lagemaat, S. O. Kelley, E. H. Sargent, *Joule* **2018**, *2*, 825.
[9] Y. Li, W. Shan, M. J. Zachman, M. Wang, S. Hwang, H. Tabassum, J. Yang, X. Yang, S. Karakalos, Z. Feng, G. Wang, G. Wu, *Angew. Chem., Int. Ed.* **2022**, *61*, 202205632.
[10] S. Jin, Y. Ni, Z. Hao, K. Zhang, Y. Lu, Z. Yan, Y. Wei, Y.-R. Lu, T.-S. Chan, J. Chen, *Angew. Chem., Int. Ed.* **2020**, *59*, 21885.
[11] X. Wang, Y. Wang, X. Sang, W. Zheng, S. Zhang, L. Shuai, B. Yang, Z. Li, J. Chen, L. Lei, N. M. Adli, M. K. H. Leung, M. Qiu, G. Wu, Y. Hou, *Angew. Chem., Int. Ed.* **2021**, *60*, 4192.
[12] S. Jin, Z. Hao, K. Zhang, Z. Yan, J. Chen, *Angew. Chem., Int. Ed.* **2021**, *60*, 20627.
[13] C. Chen, J. F. Khosrowabadi Kotyk, S. W. Sheehan, *Chem* **2018**, *4*, 2571.
[14] M. Jouny, W. Luc, F. Jiao, *Ind. Eng. Chem. Res.* **2018**, *57*, 2165.
[15] S. Sultan, H. Lee, S. Park, M. M. Kim, A. Yoon, H. Choi, T.-H. Kong, Y.-J. Koe, H.-S. Oh, Z. Lee, H. Kim, W. Kim, Y. Kwon, *Energy Environ. Sci.* **2022**, *15*, 2397.
[16] F. P. García de Arquer, C.-T. Dinh, A. Ozden, J. Wicks, C. McCallum, A. R. Kirmani, D.-H. Nam, C. Gabardo, A. Seifitokaldani, X. Wang, Y. C. Li, F. Li, J. Edwards, L. J. Richter, S. J. Thorpe, D. Sinton, E. H. Sargent, *Science* **2020**, *367*, 661.
[17] J. M. Spurgeon, B. Kumar, *Energy Environ. Sci.* **2018**, *11*, 1536.
[18] M. G. Kibria, J. P. Edwards, C. M. Gabardo, C.-T. Dinh, A. Seifitokaldani, D. Sinton, E. H. Sargent, *Adv. Mater.* **2019**, *31*, 1807166.
[19] H. Yoshio, K. Katsuhei, M. Akira, S. Shin, *Chem. Lett.* **1986**, *15*, 897.
[20] H. Yoshio, K. Katsuhei, S. Shin, *Chem. Lett.* **1985**, *14*, 1695.
[21] J. Santatiwongchai, K. Faungnawakij, P. Hirunsit, *ACS Catal.* **2021**, *11*, 9688.
[22] T. K. Todorova, M. W. Schreiber, M. Fontecave, *ACS Catal.* **2020**, *10*, 1754.
[23] H. H. Heenen, H. Shin, G. Kastlunger, S. Overa, J. A. Gauthier, F. Jiao, K. Chan, *Energy Environ. Sci.* **2022**, *15*, 3978.
[24] K. P. Kuhl, E. R. Cave, D. N. Abram, T. F. Jaramillo, *Energy Environ. Sci.* **2012**, *5*, 7050.
[25] K. P. Kuhl, T. Hatsukade, E. R. Cave, D. N. Abram, J. Kibsgaard, T. F. Jaramillo, *J. Am. Chem. Soc.* **2014**, *136*, 14107.
[26] X. Zhao, L. Du, B. You, Y. Sun, *Catal. Sci. Technol.* **2020**, *10*, 2711.
[27] G. Mangione, J. Huang, R. Buonsanti, C. Corminboeuf, *J. Phys. Chem. Lett.* **2019**, *10*, 4259.
[28] Y. Li, H. S. Pillai, T. Wang, S. Hwang, Y. Zhao, Z. Qiao, Q. Mu, S. Karakalos, M. Chen, J. Yang, D. Su, H. Xin, Y. Yan, G. Wu, *Energy Environ. Sci.* **2021**, *14*, 1449.

[29] X. Lv, Z. Liu, C. Yang, Y. Ji, G. Zheng, *Acc Mater Res* **2023**, *4*, 264.
[30] J. Pérez-Ramírez, N. López, *Nat. Catal.* **2019**, *2*, 971.
[31] F. Pan, Y. Yang, *Energy Environ. Sci.* **2020**, *13*, 2275.
[32] W. Nie, C. C. L. McCrory, *Dalton Trans.* **2022**, *51*, 6993.
[33] Y. Li, Y. Chen, Z. Guo, C. Tang, B. Sa, N. Miao, J. Zhou, Z. Sun, *Chem. Eng. J.* **2022**, *429*, 132171.
[34] N. Govindarajan, J. M. García-Lastra, E. J. Meijer, F. Calle-Vallejo, *Curr. Opin. Electrochem.* **2018**, *8*, 110.
[35] Y. Kang, F. Zhang, B. Liu, Y. Sun, X. Zhang, W. Song, Y. Wei, Z. Zhao, J. Liu, *Phys. Chem. Chem. Phys.* **2020**, *22*, 18672.
[36] C. Fu, T. O'Carroll, S. Shen, L. Luo, J. Zhang, H. Xu, G. Wu, *Curr. Opin. Electrochem.* **2023**, *38*, 101227.
[37] X. Li, S. Duan, E. Sharman, Y. Zhao, L. Yang, Z. Zhuo, P. Cui, J. Jiang, Y. Luo, *J. Mater. Chem. A* **2020**, *8*, 10193.
[38] J. H. Montoya, C. Tsai, A. Vojvodic, J. K. Nørskov, *ChemSusChem* **2015**, *8*, 2180.
[39] M. Andersen, S. V. Levchenko, M. Scheffler, K. Reuter, *ACS Catal.* **2019**, *9*, 2752.
[40] J. Na, B. Seo, J. Kim, C. W. Lee, H. Lee, Y. J. Hwang, B. K. Min, D. K. Lee, H.-S. Oh, U. Lee, *Nat. Commun.* **2019**, *10*, 5193.
[41] X. Chen, J. Chen, N. M. Alghoraibi, D. A. Henckel, R. Zhang, U. O. Nwabara, K. E. Madsen, P. J. A. Kenis, S. C. Zimmerman, A. A. Gewirth, *Nat. Catal.* **2021**, *4*, 20.
[42] B. Zhang, J. Zhang, M. Hua, Q. Wan, Z. Su, X. Tan, L. Liu, F. Zhang, G. Chen, D. Tan, X. Cheng, B. Han, L. Zheng, G. Mo, *J. Am. Chem. Soc.* **2020**, *142*, 13606.
[43] S. Li, H. Duan, J. Yu, C. Qiu, R. Yu, Y. Chen, Y. Fang, X. Cai, S. Yang, *ACS Catal.* **2022**, *12*, 9074.
[44] X. Ma, Y. Zhang, T. Fan, D. Wei, Z. Huang, Z. Zhang, Z. Zhang, Y. Dong, Q. Hong, Z. Chen, X. Yi, *Adv. Funct. Mater.* **2023**, *33*, 2213145.
[45] I. V. Chernyshova, P. Somasundaran, S. Ponnurangam, *Proc. Natl. Acad. Sci. USA* **2018**, *115*, E9261.
[46] C. F. Wen, F. Mao, Y. Liu, X. Y. Zhang, H. Q. Fu, L. R. Zheng, P. F. Liu, H. G. Yang, *ACS Catal.* **2020**, *10*, 1086.
[47] W. Ren, X. Tan, W. Yang, C. Jia, S. Xu, K. Wang, S. C. Smith, C. Zhao, *Angew. Chem., Int. Ed.* **2019**, *58*, 6972.
[48] L. Fan, C. Xia, P. Zhu, Y. Lu, H. Wang, *Nat. Commun.* **2020**, *11*, 3633.
[49] X. Zong, Y. Jin, C. Liu, Y. Yao, J. Zhang, W. Luo, A. Züttel, Y. Xiong, *Electrochem. Commun.* **2021**, *124*, 106968.
[50] A. Bagger, W. Ju, A. S. Varela, P. Strasser, J. Rossmeisl, *ChemPhysChem* **2017**, *18*, 3266.
[51] R. Kortlever, J. Shen, K. J. P. Schouten, F. Calle-Vallejo, M. T. M. Koper, *J. Phys. Chem. Lett.* **2015**, *6*, 4073.
[52] K. J. P. Schouten, Y. Kwon, C. J. M. van der Ham, Z. Qin, M. T. M. Koper, *Chem. Sci.* **2011**, *2*, 1902.
[53] J. Hussain, H. Jónsson, E. Skúlason, *ACS Catal.* **2018**, *8*, 5240.
[54] W. Ma, S. Xie, T. Liu, Q. Fan, J. Ye, F. Sun, Z. Jiang, Q. Zhang, J. Cheng, Y. Wang, *Nat. Catal.* **2020**, *3*, 478.
[55] C. Zhan, F. Dattila, C. Rettenmaier, A. Bergmann, S. Kühl, R. García-Muelas, N. López, B. R. Cuenya, *ACS Catal.* **2021**, *11*, 7694.
[56] Y. Dai, H. Li, C. Wang, W. Xue, M. Zhang, D. Zhao, J. Xue, J. Li, L. Luo, C. Liu, X. Li, P. Cui, Q. Jiang, T. Zheng, S. Gu, Y. Zhang, J. Xiao, C. Xia, J. Zeng, *Nat. Commun.* **2023**, *14*, 3382.
[57] F. Pan, L. Fang, B. Li, X. Yang, T. O'Carroll, H. Li, T. Li, G. Wang, K.-J. Chen, G. Wu, *J. Am. Chem. Soc.* **2024**, *146*, 1423.
[58] X. Wang, A. Xu, F. Li, S.-F. Hung, D.-H. Nam, C. M. Gabardo, Z. Wang, Y. Xu, A. Ozden, A. S. Rasouli, A. H. Ip, D. Sinton, E. H. Sargent, *J. Am. Chem. Soc.* **2020**, *142*, 3525.
[59] H. Hu, S. Qian, Q. Shi, M. Du, N. Sun, Y. Ding, J. Li, Q. Luo, Z. Li, L. He, Y. Sun, Y. Li, *ACS Appl. Mater. Interfaces* **2024**, *16*, 22025.
[60] T. Zhang, Y. Jin, S. N. Lou, T. Yan, T. Xiao, Z. Liu, J. Lin, S. Kuang, S. Zhang, X. Ma, *Appl. Catal. B: Environ. and Energy* **2024**, *353*, 124065.
[61] J. Wang, M. Sun, H. Xu, F. Hao, Q. Wa, J. Su, J. Zhou, Y. Wang, J. Yu, P. Zhang, R. Ye, S. Chu, B. Huang, M. Shao, Z. Fan, *ACS Nano* **2024**, *18*, 7192.
[62] J. Wicks, M. L. Jue, V. A. Beck, J. S. Oakdale, N. A. Dudukovic, A. L. Clemens, S. Liang, M. E. Ellis, G. Lee, S. E. Baker, E. B. Duoss, E. H. Sargent, *Adv. Mater.* **2021**, *33*, 2003855.
[63] J. Li, A. Ozden, M. Wan, Y. Hu, F. Li, Y. Wang, R. R. Zamani, D. Ren, Z. Wang, Y. Xu, D.-H. Nam, J. Wicks, B. Chen, X. Wang, M. Luo, M. Graetzel, F. Che, E. H. Sargent, D. Sinton, *Nat. Commun.* **2021**, *12*, 2808.
[64] H. Wu, L. Huang, J. Timoshenko, K. Qi, W. Wang, J. Liu, Y. Zhang, S. Yang, E. Petit, V. Flaud, J. Li, C. Salameh, P. Miele, L. Lajaunie, B. Roldán Cuenya, D. Rao, D. Voiry, *Nat. Energy* **2024**, *9*, 422.
[65] F. Li, A. Thevenon, A. Rosas-Hernández, Z. Wang, Y. Li, C. M. Gabardo, A. Ozden, C. T. Dinh, J. Li, Y. Wang, J. P. Edwards, Y. Xu, C. McCallum, L. Tao, Z.-Q. Liang, M. Luo, X. Wang, H. Li, C. P. O'Brien, C.-S. Tan, D.-H. Nam, R. Quintero-Bermudez, T.-T. Zhuang, Y. C. Li, Z. Han, R. D. Britt, D. Sinton, T. Agapie, J. C. Peters, E. H. Sargent, *Nature* **2020**, *577*, 509.
[66] J. Li, Z. Wang, C. McCallum, Y. Xu, F. Li, Y. Wang, C. M. Gabardo, C.-T. Dinh, T.-T. Zhuang, L. Wang, J. Y. Howe, Y. Ren, E. H. Sargent, D. Sinton, *Nat. Catal.* **2019**, *2*, 1124.
[67] S. Popovic, M. Smiljanic, P. Jovanovic, J. Vavra, R. Buonsanti, N. Hodnik, *Angew. Chem., Int. Ed.* **2020**, *59*, 14736.
[68] X. Wang, J. F. de Araújo, W. Ju, A. Bagger, H. Schmies, S. Kühl, J. Rossmeisl, P. Strasser, *Nat. Nanotechnol.* **2019**, *14*, 1063.
[69] G. M. Tomboc, S. Choi, T. Kwon, Y. J. Hwang, K. Lee, *Adv. Mater.* **2020**, *32*, 1908398.
[70] F. Scholten, K.-L. C. Nguyen, J. P. Bruce, M. Heyde, B. Roldan Cuenya, *Angew. Chem., Int. Ed.* **2021**, *60*, 19169.
[71] D. Zhong, Z.-J. Zhao, Q. Zhao, D. Cheng, B. Liu, G. Zhang, W. Deng, H. Dong, L. Zhang, J. Li, J. Li, J. Gong, *Angew. Chem., Int. Ed.* **2021**, *60*, 4879.
[72] A. Loiudice, P. Lobaccaro, E. A. Kamali, T. Thao, B. H. Huang, J. W. Ager, R. Buonsanti, *Angew. Chem., Int. Ed.* **2016**, *55*, 5789.
[73] H. Zhang, Y. Qiao, Y. Wang, Y. Zheng, H. Huang, *Sustainable Energy Fuels* **2022**, *6*, 4860.
[74] W. Fang, R. Lu, F.-M. Li, C. He, D. Wu, K. Yue, Y. Mao, W. Guo, B. You, F. Song, T. Yao, Z. Wang, B. Y. Xia, *Angew. Chem., Int. Ed.* **2024**, *63*, 202319936.
[75] M. Li, T. Li, C. Sun, Y. Li, P. Wan, J. Qin, R. Gao, Y. Lv, Y. Song, *Mater. Today Energy* **2024**, *42*, 101568.
[76] T. T. H. Hoang, S. Verma, S. Ma, T. T. Fister, J. Timoshenko, A. I. Frenkel, P. J. A. Kenis, A. A. Gewirth, *J. Am. Chem. Soc.* **2018**, *140*, 5791.
[77] X. Chen, Y. Zhao, J. Han, Y. Bu, *ChemPlusChem* **2023**, *88*, 202200370.
[78] H. Xiao, T. Cheng, W. A. Goddard, R. Sundararaman, *J. Am. Chem. Soc.* **2016**, *138*, 483.
[79] E. Pérez-Gallent, M. C. Figueiredo, F. Calle-Vallejo, M. T. M. Koper, *Angew. Chem., Int. Ed.* **2017**, *56*, 3621.
[80] Z. Li, P. Wang, X. Lyu, V. K. R. Kondapalli, S. Xiang, J. D. Jimenez, L. Ma, T. Ito, T. Zhang, J. Raj, Y. Fang, Y. Bai, J. Li, A. Serov, V. Shanov, A. I. Frenkel, S. D. Senanayake, S. Yang, T. P. Senftle, J. Wu, *Nature Chem. Eng.* **2024**, *1*, 159.
[81] H. Zhang, X. Wang, Y. Sun, X. Wang, Z. Tang, S. Li, X. Gao, J. Wang, Z. Hou, K. Nie, J. Xie, Z. Yang, Y.-M. Yan, *Appl. Catal. B: Environ. and Energy* **2024**, *351*, 123992.
[82] J. Li, Y. Chen, B. Yao, W. Yang, X. Cui, H. Liu, S. Dai, S. Xi, Z. Sun, W. Chen, Y. Qin, J. Wang, Q. He, C. Ling, D. Wang, Z. Zhang, *J. Am. Chem. Soc.* **2024**, *146*, 5693.
[83] Y. Zhang, F. Chen, X. Hao, Y. Liu, W. Wu, X. Zhang, Z. Zang, H. Dong, W. Wang, F. Lu, Z. Lu, H. Liu, H. Liu, F. Luo, Y. Cheng, *Appl. Catal. B: Environ. and Energy* **2024**, *344*, 123666.

[84] X. Xu, D. Xiao, Y. Gao, W. Li, M. Gao, S. Zhao, Z. Wang, Z. Zheng, P. Wang, H. Cheng, Y. Liu, Y. Dai, B. Huang, *ACS Appl. Mater. Interfaces* **2024**, *16*, 16243.
[85] F. Calle-Vallejo, M. T. M. Koper, *Angew. Chem., Int. Ed.* **2013**, *52*, 7282.
[86] T. Cheng, H. Xiao, W. A. Goddard, *Proc. Natl. Acad. Sci. USA* **2017**, *114*, 1795.
[87] Y. Lin, T. Wang, L. Zhang, G. Zhang, L. Li, Q. Chang, Z. Pang, H. Gao, K. Huang, P. Zhang, Z.-J. Zhao, C. Pei, J. Gong, *Nat. Commun.* **2023**, *14*, 3575.
[88] F. Calle-Vallejo, M. T. M. Koper, *ACS Catal.* **2017**, *7*, 7346.
[89] K. Rossi, R. Buonsanti, *Acc. Chem. Res.* **2022**, *55*, 629.
[90] L. Zaza, K. Rossi, R. Buonsanti, *ACS Energy Lett.* **2022**, *7*, 1284.
[91] J. Zhang, G. Zeng, S. Zhu, H. Tao, Y. Pan, W. Lai, J. Bao, C. Lian, D. Su, M. Shao, H. Huang, *Proc. Natl. Acad. Sci. USA* **2023**, *120*, 2218987120.
[92] D.-J. Su, S.-Q. Xiang, S.-T. Gao, Y. Jiang, X. Liu, W. Zhang, L.-B. Zhao, Z.-Q. Tian, *JACS Au* **2023**, *3*, 905.
[93] D. Ren, J. Fong, B. S. Yeo, *Nat. Commun.* **2018**, *9*, 925.
[94] D. A. Henckel, M. J. Counihan, H. E. Holmes, X. Chen, U. O. Nwabara, S. Verma, J. Rodríguez-López, P. J. A. Kenis, A. A. Gewirth, *ACS Catal.* **2021**, *11*, 255.
[95] S. E. Weitzner, S. A. Akhade, J. B. Varley, B. C. Wood, M. Otani, S. E. Baker, E. B. Duoss, *J. Phys. Chem. Lett.* **2020**, *11*, 4113.
[96] W. Liu, P. Zhai, A. Li, B. Wei, K. Si, Y. Wei, X. Wang, G. Zhu, Q. Chen, X. Gu, R. Zhang, W. Zhou, Y. Gong, *Nat. Commun.* **2022**, *13*, 1877.
[97] C.-T. Dinh, T. Burdyny, M. G. Kibria, A. Seifitokaldani, C. M. Gabardo, F. P. García de Arquer, A. Kiani, J. P. Edwards, P. De Luna, O. S. Bushuyev, C. Zou, R. Quintero-Bermudez, Y. Pang, D. Sinton, E. H. Sargent, *Science* **2018**, *360*, 783.
[98] S. Popovic, M. Bele, N. Hodnik, *ChemElectroChem* **2021**, *8*, 2634.
[99] D. Ma, T. Jin, K. Xie, H. Huang, *J. Mater. Chem. A* **2021**, *9*, 20897.
[100] J. Huang, N. Hörmann, E. Oveisi, A. Loiudice, G. L. De Gregorio, O. Andreussi, N. Marzari, R. Buonsanti, *Nat. Commun.* **2018**, *9*, 3117.
[101] R. M. Arán-Ais, F. Scholten, S. Kunze, R. Rizo, B. Roldan Cuenya, *Nat. Energy* **2020**, *5*, 317.
[102] J. Kim, W. Choi, J. W. Park, C. Kim, M. Kim, H. Song, *J. Am. Chem. Soc.* **2019**, *141*, 6986.
[103] J. Zhang, Z. Liu, H. Guo, H. Lin, H. Wang, X. Liang, H. Hu, Q. Xia, X. Zou, X. Huang, *ACS Appl. Mater. Interfaces* **2022**, *14*, 19388.
[104] Y. Jännsch, M. Hämmerle, E. Simon, M. Fleischer, R. Moos, *Energy Technol.* **2022**, *10*, 2200046.
[105] D. Gao, I. Sinev, F. Scholten, R. M. Arán-Ais, N. J. Divins, K. Kvashnina, J. Timoshenko, B. Roldan Cuenya, *Angew. Chem., Int. Ed.* **2019**, *58*, 17047.
[106] M. Li, M. N. Idros, Y. Wu, T. Burdyny, S. Garg, X. S. Zhao, G. Wang, T. E. Rufford, *J. Mater. Chem. A* **2021**, *9*, 19369.
[107] Y. Wu, S. Garg, M. Li, M. N. Idros, Z. Li, R. Lin, J. Chen, G. Wang, T. E. Rufford, *J. Power Sources* **2022**, *522*, 230998.
[108] K. Yang, R. Kas, W. A. Smith, T. Burdyny, *ACS Energy Lett* **2021**, *6*, 33.
[109] D. Salvatore, C. P. Berlinguette, *ACS Energy Lett.* **2020**, *5*, 215.
[110] A. Ozden, F. Li, F. P. Garci?a de Arquer, A. Rosas-Hernández, A. Thevenon, Y. Wang, S.-F. Hung, X. Wang, B. Chen, J. Li, J. Wicks, M. Luo, Z. Wang, T. Agapie, J. C. Peters, E. H. Sargent, D. Sinton, *ACS Energy Lett* **2020**, *5*, 2811.
[111] L.-C. Weng, A. T. Bell, A. Z. Weber, *Energy Environ. Sci.* **2019**, *12*, 1950.
[112] D. A. Salvatore, C. M. Gabardo, A. Reyes, C. P. O'Brien, S. Holdcroft, P. Pintauro, B. Bahar, M. Hickner, C. Bae, D. Sinton, E. H. Sargent, C. P. Berlinguette, *Nat. Energy* **2021**, *6*, 339.
[113] Y. Xu, J. P. Edwards, S. Liu, R. K. Miao, J. E. Huang, C. M. Gabardo, C. P. O'Brien, J. Li, E. H. Sargent, D. Sinton, *ACS Energy Lett.* **2021**, *6*, 809.
[114] A. K. Buckley, M. Lee, T. Cheng, R. V. Kazantsev, D. M. Larson, W. A. Goddard III, F. D. Toste, F. M. Toma, *J. Am. Chem. Soc.* **2019**, *141*, 7355.
[115] F. S. Roberts, K. P. Kuhl, A. Nilsson, *Angew. Chem., Int. Ed.* **2015**, *54*, 5179.
[116] K. Liu, W. A. Smith, T. Burdyny, *ACS Energy Lett.* **2019**, *4*, 639.
[117] D.-H. Nam, O. Shekhah, A. Ozden, C. McCallum, F. Li, X. Wang, Y. Lum, T. Lee, J. Li, J. Wicks, A. Johnston, D. Sinton, M. Eddaoudi, E. H. Sargent, *Adv. Mater.* **2022**, *34*, 2207088.
[118] B. Sahin, J. J. Leung, E. Magori, S. Laumen, A. Tawil, E. Simon, O. Hinrichsen, *Energy Technol.* **2022**, *10*, 2200972.
[119] M. Etzi, J. Dangbegnon, A. Chiodoni, C. F. Pirri, *J. CO2 Util.* **2024**, *83*, 102772.
[120] M. Sassenburg, M. Kelly, S. Subramanian, W. A. Smith, T. Burdyny, *ACS Energy Lett.* **2023**, *8*, 321.
[121] K. V. Petrov, J. C. Bui, L. Baumgartner, L.-C. Weng, S. M. Dischinger, D. M. Larson, D. J. Miller, A. Z. Weber, D. A. Vermaas, *Sustainable Energy Fuels* **2022**, *6*, 5077.
[122] R. B. Kutz, Q. Chen, H. Yang, S. D. Sajjad, Z. Liu, I. R. Masel, *Energy Technol.* **2017**, *5*, 929.
[123] P. Wei, H. Li, L. Lin, D. Gao, X. Zhang, H. Gong, G. Qing, R. Cai, G. Wang, X. Bao, *Sci. China: Chem.* **2020**, *63*, 1711.
[124] B. M. Carter, L. Keller, M. Wessling, D. J. Miller, *J. Mater. Chem. A.* **2019**, *7*, 23818.
[125] M. Krödel, B. M. Carter, D. Rall, J. Lohaus, M. Wessling, D. J. Miller, *ACS Appl. Mater. Interfaces* **2020**, *12*, 12030.
[126] J. Zhang, W. Luo, A. Züttel, *J. Catal.* **2020**, *385*, 140.
[127] G. O. Larrazábal, P. Strøm-Hansen, J. P. Heli, K. Zeiter, K. T. Therkildsen, I. Chorkendorff, B. Seger, *ACS Appl. Mater. Interfaces* **2019**, *11*, 41281.
[128] C. McCallum, C. M. Gabardo, C. P. O'Brien, J. P. Edwards, J. Wicks, Y. Xu, E. H. Sargent, D. Sinton, *Cell Rep. Phys. Sci.* **2021**, *2*, 100522.
[129] M. Ma, S. Kim, I. Chorkendorff, B. Seger, *Chem. Sci.* **2020**, *11*, 8854.
[130] T. Alkayyali, A. S. Zeraati, H. Mar, F. Arabyarmohammadi, S. Saber, R. K. Miao, C. P. O'Brien, H. Liu, Z. Xie, G. Wang, E. H. Sargent, N. Zhao, D. Sinton, *ACS Energy Lett.* **2023**, *8*, 4674.
[131] B. De Mot, J. Hereijgers, N. Daems, T. Breugelmans, *Chem. Eng. J.* **2022**, *428*, 131170.
[132] D. A. Salvatore, D. M. Weekes, J. He, K. E. Dettelbach, Y. C. Li, T. E. Mallouk, C. P. Berlinguette, *ACS Energy Lett.* **2018**, *3*, 149.
[133] M. W. Schreiber, *Curr Opin Electrochem* **2024**, *44*, 101438.
[134] K. Xie, R. K. Miao, A. Ozden, S. Liu, Z. Chen, C.-T. Dinh, J. E. Huang, Q. Xu, C. M. Gabardo, G. Lee, J. P. Edwards, C. P. O'Brien, S. W. Boettcher, D. Sinton, E. H. Sargent, *Nat. Commun.* **2022**, *13*, 3609.
[135] X. She, L. Zhai, Y. Wang, P. Xiong, M. M.-J. Li, T.-S. Wu, M. C. Wong, X. Guo, Z. Xu, H. Li, H. Xu, Y. Zhu, S. C. E. Tsang, S. P. Lau, *Nat. Energy* **2024**, *9*, 81.
[136] W. H. Lee, C. Lim, S. Y. Lee, K. H. Chae, C. H. Choi, U. Lee, B. K. Min, Y. J. Hwang, H.-S. Oh, *Nano Energy* **2021**, *84*, 105859.
[137] Z. Wang, Y. Li, X. Zhao, S. Chen, Q. Nian, X. Luo, J. Fan, D. Ruan, B.-Q. Xiong, X. Ren, *J. Am. Chem. Soc.* **2023**, *145*, 6339.
[138] Z. Jiang, Z. Zhang, H. Li, Y. Tang, Y. Yuan, J. Zao, H. Zheng, Y. Liang, *Adv. Energy Mater.* **2023**, *13*, 2203603.
[139] A. R. Heenan, J. Hamonnet, A. T. Marshall, *ACS Energy Lett.* **2022**, *7*, 2357.
[140] Z. Zhang, L. Melo, R. P. Jansonius, F. Habibzadeh, E. R. Grant, C. P. Berlinguette, *ACS Energy Lett.* **2020**, *5*, 3101.
[141] X. Cheng, Z. Shi, N. Glass, L. Zhang, J. Zhang, D. Song, Z.-S. Liu, H. Wang, J. Shen, *J. Power Sources* **2007**, *165*, 739.
[142] L. Dubau, L. Castanheira, F. Maillard, M. Chatenet, O. Lottin, G. Maranzana, J. Dillet, A. Lamibrac, J.-C. Perrin, E. Moukheiber, A. ElKaddouri, G. De Moor, C. Bas, L. Flandin, N. Caqué, *Wiley Interdiscip Rev Energy Environ* **2014**, *3*, 540.

[143] K. Scott, W. M. Taama, P. Argyropoulos, K. Sundmacher, *J. Power Sources* **1999**, *83*, 204.
[144] V. A. Paganin, E. Sitta, T. Iwasita, W. Vielstich, *J. Appl. Electrochem.* **2005**, *35*, 1239.
[145] C. Wang, A. Schechter, L. Feng, *Nano Research Energy* **2023**, *2*, 9120056.
[146] T. Reier, M. Oezaslan, P. Strasser, *ACS Catal.* **2012**, *2*, 1765.
[147] C. Feng, M. B. Faheem, J. Fu, Y. Xiao, C. Li, Y. Li, *ACS Catal.* **2020**, *10*, 4019.
[148] Y. Gao, L. Neal, D. Ding, W. Wu, C. Baroi, A. M. Gaffney, F. Li, *ACS Catal.* **2019**, *9*, 8592.
[149] B. Alonso-Fariñas, A. Gallego-Schmid, P. Haro, A. Azapagic, *J. Cleaner Prod.* **2018**, *202*, 817.
[150] S. Verma, B. Kim, H.-R. "M." Jhong, S. Ma, P. J. A. Kenis, *ChemSusChem* **2016**, *9*, 1972.
[151] J. G. de Vries, *Curr Opin Green Sustain Chem* **2023**, *39*, 100715.
[152] Z. Zhao, K. Chong, J. Jiang, K. Wilson, X. Zhang, F. Wang, *Renewable Sustainable Energy Rev.* **2018**, *97*, 580.
[153] T. Alerte, A. Gaona, J. P. Edwards, C. M. Gabardo, C. P. O'Brien, J. Wicks, L. Bonnenfant, A. S. Rasouli, D. Young, J. Abed, L. Kershaw, Y. C. Xiao, A. Sarkar, S. A. Jaffer, M. W. Schreiber, D. Sinton, H. L. MacLean, E. H. Sargent, *ACS Sustainable Chem. Eng.* **2023**, *11*, 15651.
[154] A. Ozden, Y. Wang, F. Li, M. Luo, J. Sisler, A. Thevenon, A. Rosas-Hernández, T. Burdyny, Y. Lum, H. Yadegari, T. Agapie, J. C. Peters, E. H. Sargent, D. Sinton, *Joule* **2021**, *5*, 706.
[155] K. Xie, A. Ozden, R. K. Miao, Y. Li, D. Sinton, E. H. Sargent, *Nat. Commun.* **2022**, *13*, 3070.
[156] F. Chang, G. Zhan, Z. Wu, Y. Duan, S. Shi, S. Zeng, X. Zhang, S. Zhang, *ACS Sustainable Chem. Eng.* **2021**, *9*, 9045.
[157] S. Mavrikis, M. Nieuwoudt, M. Göltz, S. Ehles, A. Körner, A. Hutzler, E. Fossy, A. Zervas, O. Brai, M. Wegener, F. Doerrfuss, P. Bouwman, S. Rosiwal, L. Wang, C. Ponce de León, *Adv. Energy Mater.* **2024**, *14*, 2304247.
[158] R. Zhao, Y. Wang, G. Ji, F. Zhang, Y. Wang, Y. Zhao, B. Han, Z. Liu, *Chem. Eng. J.* **2024**, *486*, 150280.
[159] E. Ruiz-López, J. Gandara-Loe, F. Baena-Moreno, T. R. Reina, J. A. Odriozola, *Renewable Sustainable Energy Rev.* **2022**, *161*, 112329.
[160] M. Pérez-Fortes, A. Bocin-Dumitriu, E. Tzimas, *Energy Procedia* **2014**, *63*, 7968.
[161] J. Kim, C. A. Henao, T. A. Johnson, D. E. Dedrick, J. E. Miller, E. B. Stechel, C. T. Maravelias, *Energy Environ. Sci.* **2011**, *4*, 3122.
[162] J. Sisler, S. Khan, A. H. Ip, M. W. Schreiber, S. A. Jaffer, E. R. Bobicki, C.-T. Dinh, E. H. Sargent, *ACS Energy Lett.* **2021**, *6*, 997.
[163] A. H. Nyhus, M. Yliruka, N. Shah, B. Chachuat, *Energy Environ. Sci.* **2024**, *17*, 1931.
[164] T. Gao, B. Xia, K. Yang, D. Li, T. Shao, S. Chen, Q. Li, J. Duan, *Energy Fuels* **2023**, *37*, 17997.
[165] Y.-J. Ko, C. Lim, J. Jin, M. G. Kim, J. Y. Lee, T.-Y. Seong, K.-Y. Lee, B. K. Min, J.-Y. Choi, T. Noh, G. W. Hwang, W. H. Lee, H.-S. Oh, *Nat. Commun.* **2024**, *15*, 3356.
[166] Y. Li, H. Wang, X. Yang, T. O'Carroll, G. Wu, *Angew. Chem., Int. Ed.* **2024**, *63*, 202317884.
[167] J. Yu, J. Xiao, Y. Ma, J. Zhou, P. Lu, K. Wang, Y. Yan, J. Zeng, Y. Wang, S. Song, Z. Fan, *Chem Catalysis* **2023**, *3*, 100670.
[168] Y. Chen, X.-Y. Li, Z. Chen, A. Ozden, J. E. Huang, P. Ou, J. Dong, J. Zhang, C. Tian, B.-H. Lee, X. Wang, S. Liu, Q. Qu, S. Wang, Y. Xu, R. K. Miao, Y. Zhao, Y. Liu, C. Qiu, J. Abed, H. Liu, H. Shin, D. Wang, Y. Li, D. Sinton, E. H. Sargent, *Nat. Nanotechnol.* **2024**, *19*, 311.
[169] M. Zheng, P. Wang, X. Zhi, K. Yang, Y. Jiao, J. Duan, Y. Zheng, S.-Z. Qiao, *J. Am. Chem. Soc.* **2022**, *144*, 14936.
[170] H. Shin, K. U. Hansen, F. Jiao, *Nat. Sustain.* **2021**, *4*, 911.
[171] T. Alkayyali, M. Zargartalebi, A. Ozden, F. Arabyarmohammadi, R. Dorakhan, J. P. Edwards, F. Li, A. Shayesteh Zeraati, M. Fan, A. Bazylak, E. H. Sargent, D. Sinton, *Joule* **2024**, *8*, 1478.
[172] A. Ozden, J. Li, S. Kandambeth, X.-Y. Li, S. Liu, O. Shekhah, P. Ou, Y. Zou Finfrock, Y.-K. Wang, T. Alkayyali, F. Pelayo García de Arquer, V. S. Kale, P. M. Bhatt, A. H. Ip, M. Eddaoudi, E. H. Sargent, D. Sinton, *Nat. Energy* **2023**, *8*, 179.
[173] Y. Li, Y. Li, L. Yu, Q. Hu, Q. Wang, K. Maliutina, L. Fan, *J. Power Sources* **2021**, *491*, 229599.
[174] P.-F. Sui, M.-R. Gao, Y.-C. Wang, J.-L. Luo, *Acc Mater Res* **2024**, https://doi.org/10.1021/accountsmr.3c00224.
[175] M. Ramdin, B. De Mot, A. R. T. Morrison, T. Breugelmans, L. J. P. van den Broeke, J. P. M. Trusler, R. Kortlever, W. de Jong, O. A. Moultos, P. Xiao, P. A. Webley, T. J. H. Vlugt, *Ind. Eng. Chem. Res.* **2021**, *60*, 17862.
[176] A. Vasileff, C. Xu, Y. Jiao, Y. Zheng, S.-Z. Qiao, *Chem* **2018**, *4*, 1809.
[177] D. Fan, S. Zhang, Y. Li, H. Bin, R. Li, Y. Li, M. An, P. Yang, J. Zhang, *J. Colloid Interface Sci.* **2024**, *662*, 786.
[178] L. Xiong, X. Zhang, H. Yuan, J. Wang, X. Yuan, Y. Lian, H. Jin, H. Sun, Z. Deng, D. Wang, J. Hu, H. Hu, J. Choi, J. Li, Y. Chen, J. Zhong, J. Guo, M. H. Rümmerli, L. Xu, Y. Peng, *Angew. Chem., Int. Ed.* **2021**, *60*, 2508.
[179] C. D. Koolen, E. Oveisi, J. Zhang, M. Li, O. V. Safonova, J. K. Pedersen, J. Rossmeisl, W. Luo, A. Züttel, *Nature Synthesis* **2023**, *3*, 47.
[180] R. Jiang, V. S. Parameshwaran, J. Boltersdorf, D. R. Baker, *ACS Appl Energy Mater* **2023**, *6*, 10475.
[181] S. Jia, Q. Zhu, H. Wu, S. Han, M. Chu, J. Zhai, X. Xing, W. Xia, M. He, B. Han, *Chem. Sci.* **2022**, *13*, 7509.
[182] S. Shen, X. Peng, L. Song, Y. Qiu, C. Li, L. Zhuo, J. He, J. Ren, X. Liu, J. Luo, *Small* **2019**, *15*, 1902229.
[183] Y. Jia, F. Li, K. Fan, L. Sun, *Adv. Powder Mater.* **2022**, *1*, 100012.
[184] Y. Baek, H. Song, D. Hong, S. Wang, S. Lee, Y.-C. Joo, G.-D. Lee, J. Oh, *J. Mater. Chem. A* **2022**, *10*, 9393.
[185] S. Juntrapirom, J. Santatiwongchai, A. Watwiangkham, S. Suthirakun, T. Butburee, K. Faungnawakij, P. Chakthranont, P. Hirunsit, B. Rungtaweevoranit, *Catal. Sci. Technol.* **2021**, *11*, 8065.
[186] B. Kim, Y. C. Tan, Y. Ryu, K. Jang, H. G. Abbas, T. Kang, H. Choi, K.-S. Lee, S. Park, W. Kim, P.-P. Choi, S. Ringe, J. Oh, *ACS Energy Lett.* **2023**, *8*, 3356.
[187] J. Y. Kim, C. H. Ryu, J. H. Lee, A. U. Pawar, W.-D. Jang, Y. S. Kang, H. S. Ahn, *ACS Appl Energy Mater* **2020**, *3*, 6670.
[188] Y. Li, Z. Tian, L. Chen, *J. Phys. Chem. C.* **2021**, *125*, 21381.
[189] Z. Zhang, X. Wang, H. Tian, H. Jiao, N. Tian, L. Bian, Y. Liu, Z.-L. Wang, *J. Colloid Interface Sci.* **2024**, *661*, 966.
[190] J.-Y. Kim, H. S. Ahn, I. Kim, D. Hong, T. Lee, J. Jo, H. Kim, M. K. Kwak, H. G. Kim, G. Kang, S. Go, W. H. Ryu, G.-D. Lee, M. Kim, D.-H. Nam, E. S. Park, Y.-C. Joo, *Nature Synthesis* **2023**, *3*, 452.
[191] D.-L. Meng, M.-D. Zhang, D.-H. Si, M.-J. Mao, Y. Hou, Y.-B. Huang, R. Cao, *Angew. Chem., Int. Ed.* **2021**, *60*, 25485.
[192] Y. Zhu, X. Cui, H. Liu, Z. Guo, Y. Dang, Z. Fan, Z. Zhang, W. Hu, *Nano Res.* **2021**, *14*, 4471.
[193] C. Kim, F. Dionigi, V. Beermann, X. Wang, T. Möller, P. Strasser, *Adv. Mater.* **2019**, *31*, 1805617.
[194] M. D. Hossain, Y. Huang, T. H. Yu, W. A. Goddard III, Z. Luo, *Nat. Commun.* **2020**, *11*, 2256.
[195] Q. Mo, S. Li, C. Chen, H. Song, Q. Gao, L. Zhang, *ACS Sustainable Chem. Eng.* **2024**, *12*, 6093.
[196] Y. Mi, S. Shen, X. Peng, H. Bao, X. Liu, J. Luo, *ChemElectroChem* **2019**, *6*, 2393.
[197] R. Yang, J. Duan, P. Dong, Q. Wen, M. Wu, Y. Liu, Y. Liu, H. Li, T. Zhai, *Angew. Chem., Int. Ed.* **2022**, *61*, 202116706.
[198] X. Yan, C. Chen, Y. Wu, Y. Chen, J. Zhang, R. Feng, J. Zhang, B. Han, *Green Chem.* **2022**, *24*, 1989.

[199] H. Li, T. Liu, P. Wei, L. Lin, D. Gao, G. Wang, X. Bao, *Angew. Chem., Int. Ed.* **2021**, *60*, 14329.
[200] Q. Wan, J. Zhang, B. Zhang, D. Tan, L. Yao, L. Zheng, F. Zhang, L. Liu, X. Cheng, B. Han, *Green Chem.* **2020**, *22*, 2750.
[201] Z. Yin, C. Yu, Z. Zhao, X. Guo, M. Shen, N. Li, M. Muzzio, J. Li, H. Liu, H. Lin, J. Yin, G. Lu, D. Su, S. Sun, *Nano Lett.* **2019**, *19*, 8658.
[202] F. Zhang, P. Wang, R. Zhao, Y. Wang, J. Wang, B. Han, Z. Liu, *ChemSusChem* **2022**, *15*, 202201267.
[203] X. Suo, F. Zhang, Z. Yang, L. Wang, M. Lei, J. A. Gaugler, M. Li, J. Fan, B. P. Thapaliya, I. Popovs, A. S. Ivanov, L. C. Gallington, D.-E. Jiang, Z. Liu, S. Dai, *Chem Catalysis* **2023**, *3*, 100506.
[204] D. Giziński, A. Brudzisz, J. S. Santos, F. Trivinho-Strixino, W. J. Stępniowski, T. Czujko, *Catalysts* **2020**, *10*, 1338.
[205] J. Timoshenko, A. Bergmann, C. Rettenmaier, A. Herzog, R. M. Arán-Ais, H. S. Jeon, F. T. Haase, U. Hejral, P. Grosse, S. Kühl, E. M. Davis, J. Tian, O. Magnussen, B. Roldan Cuenya, *Nat. Catal.* **2022**, *5*, 259.
[206] Z. Tang, E. Nishiwaki, K. E. Fritz, T. Hanrath, J. Suntivich, *ACS Appl. Mater. Interfaces* **2021**, *13*, 14050.
[207] S. T. Ahn, I. Abu-Baker, G. T. R. Palmore, *Catal. Today* **2017**, *288*, 24.
[208] C. Kim, L.-C. Weng, A. T. Bell, *ACS Catal.* **2020**, *10*, 12403.
[209] S. Y. Lee, H. Jung, N.-K. Kim, H.-S. Oh, B. K. Min, Y. J. Hwang, *J. Am. Chem. Soc.* **2018**, *140*, 8681.
[210] Q. Lei, H. Zhu, K. Song, N. Wei, L. Liu, D. Zhang, J. Yin, X. Dong, K. Yao, N. Wang, X. Li, B. Davaasuren, J. Wang, Y. Han, *J. Am. Chem. Soc.* **2020**, *142*, 4213.
[211] H. Jung, S. Y. Lee, C. W. Lee, M. K. Cho, D. H. Won, C. Kim, H.-S. Oh, B. K. Min, Y. J. Hwang, *J. Am. Chem. Soc.* **2019**, *141*, 4624.
[212] M. Fang, M. Wang, Z. Wang, Z. Zhang, H. Zhou, L. Dai, Y. Zhu, L. Jiang, *J. Am. Chem. Soc.* **2023**, *145*, 11323.
[213] Y. Wu, J. Feng, D. Shi, W. Zhang, Y. Tang, Q. Gao, *Chem. Commun.* **2023**, *59*, 10428.
[214] B. Wu, J. Chen, L. Qian, *Catalysts* **2022**, *12*, 860.
[215] Z. Zhang, L. Bian, H. Tian, Y. Liu, Y. Bando, Y. Yamauchi, Z.-L. Wang, *Small* **2022**, *18*, 2107450.
[216] Z. Han, R. Kortlever, H.-Y. Chen, J. C. Peters, T. Agapie, *ACS Cent. Sci.* **2017**, *3*, 853.
[217] M. Li, T. Li, R. Wang, C. Sun, N. Zhang, R. Gao, Y. Song, *Chem. Commun.* **2022**, *58*, 12192.
[218] B. Cheng, J. Du, H. Yuan, Y. Tao, Y. Chen, J. Lei, Z. Han, *ACS Appl. Mater. Interfaces* **2022**, *14*, 27823.
[219] Y. Qiu, H. Zhong, W. Xu, T. Zhang, X. Li, H. Zhang, *J. Mater. Chem. A* **2019**, *7*, 5453.
[220] M. S. Xie, B. Y. Xia, Y. Li, Y. Yan, Y. Yang, Q. Sun, S. H. Chan, A. Fisher, X. Wang, *Energy Environ. Sci.* **2016**, *9*, 1687.
[221] J. Wang, T. Cheng, A. Q. Fenwick, T. N. Baroud, A. Rosas-Hernández, J. H. Ko, Q. Gan, W. A. Goddard III, R. H. Grubbs, *J. Am. Chem. Soc.* **2021**, *143*, 2857.
[222] S. Banerjee, X. Han, V. S. Thoi, *ACS Catal.* **2019**, *9*, 5631.
[223] B. Deng, M. Huang, X. Zhao, S. Mou, F. Dong, *ACS Catal.* **2022**, *12*, 331.
[224] O. Christensen, S. Zhao, Z. Sun, A. Bagger, J. V. Lauritsen, S. U. Pedersen, K. Daasbjerg, J. Rossmeisl, *ACS Catal.* **2022**, *12*, 15737.
[225] L. Fan, C.-Y. Liu, P. Zhu, C. Xia, X. Zhang, Z.-Y. Wu, Y. Lu, T. P. Senftle, H. Wang, *Joule* **2022**, *6*, 205.
[226] Y. Peng, C. Zhan, H. S. Jeon, W. Frandsen, B. R. Cuenya, C. S. Kley, *ACS Appl. Mater. Interfaces* **2024**, *16*, 6562.
[227] B. Deng, X. Zhao, Y. Li, M. Huang, S. Zhang, F. Dong, *Sci. China: Chem.* **2023**, *66*, 78.
[228] H. Sun, L. Chen, L. Xiong, K. Feng, Y. Chen, X. Zhang, X. Yuan, B. Yang, Z. Deng, Y. Liu, M. H. Rümmeli, J. Zhong, Y. Jiao, Y. Peng, *Nat. Commun.* **2021**, *12*, 6823.
[229] R. Du, Q. Wu, S. Zhang, P. Wang, Z. Li, Y. Qiu, K. Yan, G. I. N. Waterhouse, P. Wang, J. Li, Y. Zhao, W.-W. Zhao, X. Wang, G. Chen, *Small* **2023**, *19*, 2301289.
[230] X. Wang, K. Klingan, M. Klingenhof, T. Möller, J. Ferreira de Araújo, I. Martens, A. Bagger, S. Jiang, J. Rossmeisl, H. Dau, P. Strasser, *Nat. Commun.* **2021**, *12*, 794.
[231] K. Yao, Y. Xia, J. Li, N. Wang, J. Han, C. Gao, M. Han, G. Shen, Y. Liu, A. Seifitokaldani, X. Sun, H. Liang, *J. Mater. Chem. A* **2020**, *8*, 11117.
[232] A. Eilert, F. Cavalca, F. S. Roberts, J. Osterwalder, C. Liu, M. Favaro, E. J. Crumlin, H. Ogasawara, D. Friebel, L. G. M. Pettersson, A. Nilsson, *J. Phys. Chem. Lett.* **2017**, *8*, 285.
[233] W. Rong, H. Zou, W. Zang, S. Xi, S. Wei, B. Long, J. Hu, Y. Ji, L. Duan, *Angew. Chem., Int. Ed.* **2021**, *60*, 466.
[234] A. Prajapati, N. C. Kani, J. A. Gauthier, R. Sartape, J. Xie, I. Bessa, M. T. Galante, S. L. Leung, M. H. S. Andrade, R. T. Somich, M. V. Rebouças, G. T. Hutras, N. Diniz, M. R. Singh, *Cell Rep. Phys. Sci.* **2022**, *3*, 101053.
[235] X. Liu, J. Li, Y. Xue, M. Gong, C. R. Cabrera, L. Yao, Z. Hu, *Fuel* **2023**, *348*, 128498.
[236] Y. Hori, A. Murata, R. Takahashi, *J. Chem. Soc., Faraday Trans. 1: Phys. Chem. in Condensed Phases* **1989**, *85*, 2309.
[237] Y. Hori, I. Takahashi, O. Koga, N. Hoshi, *J. Mol. Catal. A: Chem.* **2003**, *199*, 39.
[238] G. H. Simon, C. S. Kley, B. Roldan Cuenya, *Angew. Chem., Int. Ed.* **2021**, *60*, 2561.
[239] P. Li, D. Li, L. Liu, A. Li, C. Luo, Y. Xiao, J. Hu, H. Jiang, W. Zhang, *CrystEngComm* **2018**, *20*, 6580.
[240] J. Liu, Q. Fan, X. Chen, S. Kuang, T. Yan, H. Liu, S. Zhang, X. Ma, *Ind. Eng. Chem. Res.* **2022**, *61*, 18250.
[241] P. Grosse, A. Yoon, C. Rettenmaier, A. Herzog, S. W. Chee, B. Roldan Cuenya, *Nat. Commun.* **2021**, *12*, 6736.
[242] C. W. Li, M. W. Kanan, *J. Am. Chem. Soc.* **2012**, *134*, 7231.
[243] X. Feng, K. Jiang, S. Fan, M. W. Kanan, *ACS Cent. Sci.* **2016**, *2*, 169.
[244] Y. Li, D. Kim, S. Louisia, C. Xie, Q. Kong, S. Yu, T. Lin, S. Aloni, S. C. Fakra, P. Yang, *Proc. Natl. Acad. Sci. USA* **2020**, *117*, 9194.
[245] P.-C. Chen, C. Chen, Y. Yang, A. L. Maulana, J. Jin, J. Feijoo, P. Yang, *J. Am. Chem. Soc.* **2023**, *145*, 10116.
[246] Y. Zong, P. Chakthranont, J. Suntivich, *J. Electrochemical Energy Conversion and Storage* **2020**, *17*, 41007.
[247] A. S. Varela, M. Kroschel, T. Reier, P. Strasser, *Catal. Today* **2016**, *260*, 8.
[248] Y. Huang, C. W. Ong, B. S. Yeo, *ChemSusChem* **2018**, *11*, 3299.
[249] M. R. Singh, Y. Kwon, Y. Lum, J. W. Ager, A. T. Bell, *J. Am. Chem. Soc.* **2016**, *138*, 13006.
[250] C. M. Gabardo, A. Seifitokaldani, J. P. Edwards, C.-T. Dinh, T. Burdyny, M. G. Kibria, C. P. O'Brien, E. H. Sargent, D. Sinton, *Energy Environ. Sci.* **2018**, *11*, 2531.
[251] B. Endrodi, E. Kecsenovity, A. Samu, F. Darvas, R. V. Jones, V. Török, A. Danyi, C. Janáky, *ACS Energy Lett.* **2019**, *4*, 1770.
[252] J. P. Edwards, Y. Xu, C. M. Gabardo, C.-T. Dinh, J. Li, Z. Qi, A. Ozden, E. H. Sargent, D. Sinton, *Appl. Energy* **2020**, *261*, 114305.
[253] J. Li, Y. Kuang, Y. Meng, X. Tian, W.-H. Hung, X. Zhang, A. Li, M. Xu, W. Zhou, C.-S. Ku, C.-Y. Chiang, G. Zhu, J. Guo, X. Sun, H. Dai, *J. Am. Chem. Soc.* **2020**, *142*, 7276.
[254] N. Girichandran, S. Saedy, R. Kortlever, *Chem. Eng. J.* **2024**, *487*, 150478.
[255] R. Qiu, J. Jia, L. Peng, R. Li, S. Yan, J. Li, J. Zhang, D. T. Sun, Z. Lan, T. Xue, G. Xu, L. Cui, Z. Lv, C. Li, Y. Hong, Y. Guo, B. Ren, S. Yang, J. Li, B. Han, *Green Chem.* **2023**, *25*, 684.
[256] H. Song, J. T. Song, B. Kim, Y. C. Tan, J. Oh, *Appl. Catal., B* **2020**, *272*, 119049.
[257] L. Wang, S. A. Nitopi, E. Bertheussen, M. Orazov, C. G. Morales-Guio, X. Liu, D. C. Higgins, K. Chan, J. K. Nørskov, C. Hahn, T. F. Jaramillo, *ACS Catal.* **2018**, *8*, 7445.
[258] P. Wei, D. Gao, T. Liu, H. Li, J. Sang, C. Wang, R. Cai, G. Wang, X. Bao, *Nat. Nanotechnol.* **2023**, *18*, 299.
[259] F. Zhang, A. C. Co, *Angew. Chem., Int. Ed.* **2020**, *59*, 1674.

[260] R. M. Arán-Ais, D. Gao, B. Roldan Cuenya, *Acc. Chem. Res.* **2018**, *51*, 2906.
[261] S. Zhu, B. Jiang, W.-B. Cai, M. Shao, *J. Am. Chem. Soc.* **2017**, *139*, 15664.
[262] A. T. Chu, Y. Surendranath, *J. Am. Chem. Soc.* **2022**, *144*, 5359.
[263] Y. Xie, P. Ou, X. Wang, Z. Xu, Y. C. Li, Z. Wang, J. E. Huang, J. Wicks, C. McCallum, N. Wang, Y. Wang, T. Chen, B. T. W. Lo, D. Sinton, J. C. Yu, Y. Wang, E. H. Sargent, *Nat. Catal.* **2022**, *5*, 564.
[264] J. E. Huang, F. Li, A. Ozden, A. Sedighian Rasouli, F. P. García de Arquer, S. Liu, S. Zhang, M. Luo, X. Wang, Y. Lum, Y. Xu, K. Bertens, R. K. Miao, C.-T. Dinh, D. Sinton, E. H. Sargent, *Science* **2021**, *372*, 1074.
[265] J. Zhang, W. Cai, F. X. Hu, H. Yang, B. Liu, *Chem. Sci.* **2021**, *12*, 6800.
[266] W. H. Lee, K. Kim, C. Lim, Y.-J. Ko, Y. J. Hwang, B. K. Min, U. Lee, H.-S. Oh, *J. Mater. Chem. A* **2021**, *9*, 16169.
[267] Q. Ye, X. Zhao, R. Jin, F. Dong, H. Xie, B. Deng, *J. Mater. Chem. A* **2023**, 21498.
[268] Y. Yang, F. Li, *Curr Opin Green Sustain Chem* **2021**, *27*, 100419.
[269] Y. Yang, J. Wang, Y. Shu, Y. Ji, H. Dong, Y. Li, *Phys. Chem. Chem. Phys.* **2022**, *24*, 8591.

Thomas O' Carroll received his B.S. in Chemical and Biological Engineering from University at Buffalo before beginning work on his Ph.D. degree from the same institution under the tutelage of Dr. Gang Wu. After achieving candidacy, he transferred to working in the MPA-11: Materials Synthesis & Integrated Devices group as a graduate student at Los Alamos National Laboratory. His main focuses are the development of electrocatalytic systems for sustainability, including CO_2RR, OER, and ORR, as well as the usage of electrospinning to synthesize nanostructured catalyst supports.

Kenneth Gordon received his B.S. in Chemical Engineering and Chemistry from the University of Louisiana at Lafayette in 2022. He is pursuing his Ph.D. in Systems Engineering from the University of Louisiana at Lafayette working under Dr. Ling Fei. His research focuses on block copolymer-based materials for catalysis and energy storage applications.

Ling Fei received her B.S. in Applied Chemistry from Shantou University in 2010 and her Ph.D. in Chemical Engineering from New Mexico State University in 2014. She served as a postdoctoral researcher in the School of Chemical and Biomolecular Engineering at Cornell University from 2014 to 2016. She is currently an Assistant Professor in the Department of Chemical Engineering at The University of Louisiana at Lafayette. Her research group focuses on the design, synthesis, and engineering of nanostructured materials and their composites for various applications, including energy storage and conversion, surface coating, and catalysis.

Gang Wu is a Professor of Chemical Engineering at the University at Buffalo (UB), SUNY. He obtained his B.S. in 1997 and Ph.D. in 2004 at the Harbin Institute of Technology. After postdoctoral training at Tsinghua University, the University of South Carolina, and Los Alamos National Laboratory (LANL), he became a staff scientist at LANL in 2010. He joined UB in 2014 as an assistant professor and was promoted to a tenured associate professor in 2018 and a full professor in 2020. His research interests are advanced electrocatalysis for fuel cells, water electrolyzers, CO_2 reduction, and chemical electrosynthesis.